Running title: Pain fMRI Meta-analysis

Convergent neural representations of experimentally-induced acute pain in healthy volunteers:

A large-scale fMRI meta-analysis

Anna Xu[1], Bart Larsen[1], Erica B. Baller[1,2,3], J. Cobb Scott[1,4], Vaishnavi Sharma[1], Azeez Adebimpe[1], Allan

I. Basbaum[5], Robert H. Dworkin[6], Robert R. Edwards[7], Clifford J. Woolf[8], Simon B. Eickhoff[9,10], Claudia

R. Eickhoff[10,11], Theodore D. Satterthwaite[1*]

[1]Department of Psychiatry, University of Pennsylvania, Philadelphia PA 19104, USA
[2]Department of Psychiatry, Massachusetts General Hospital, Boston, MA, USA
[3]Department of Psychiatry, Harvard University, Boston, MA, USA
[4]VISN4 Mental Illness Research, Education, and Clinical Center at the Philadelphia VA Medical Center, Philadelphia, PA, 19104, USA
[5]Department of Anatomy, University of California, San Francisco, San Francisco, CA 94158, USA
[6]Department of Anesthesiology and Perioperative Medicine, University of Rochester School of Medicine and Dentistry, Rochester, New York
[7]Department of Anesthesiology, Perioperative and Pain Medicine, Brigham and Women's Hospital, Harvard Medical School, Boston, MA, United States
[8]FM Kirby Neurobiology Center, Boston Children's Hospital and Department of Neurobiology, Harvard Medical School, Boston, MA, USA.
[9]Institute of Systems Neuroscience, Medical Faculty, Heinrich-Heine University, D-40225 Düsseldorf, Germany
[10]Institute of Neuroscience and Medicine, Brain & Behaviour (INM-1, INM-7), Research Centre Jülich, Germany
[11]Institute of Clinical Neuroscience and Medical Psychology, Medical Faculty, Heinrich-Heine-University, 40225 Düsseldorf, Germany

Address correspondences to:

*Theodore D. Satterthwaite, Department of Psychiatry, University of Pennsylvania, 3400 Spruce St,

Philadelphia PA 19104, USA (email: sattertt@pennmedicine.upenn.edu)

Running title: Pain fMRI Meta-analysis

ABSTRACT

Characterizing a reliable, pain-related neural signature is critical for translational applications. Many prior fMRI studies have examined acute nociceptive pain-related brain activation in healthy participants. However, synthesizing these data to identify convergent patterns of activation can be challenging due to the heterogeneity of experimental designs and samples. To address this challenge, we conducted a comprehensive meta-analysis of fMRI studies of stimulus-induced pain in healthy participants. Following pre-registration, two independent reviewers evaluated 4,927 abstracts returned from a search of 8 databases, with 222 fMRI experiments meeting inclusion criteria. We analyzed these experiments using Activation Likelihood Estimation with rigorous type I error control (voxel height $p < 0.001$, cluster $p < 0.05$ FWE-corrected) and found a convergent, largely bilateral pattern of pain-related activation in the secondary somatosensory cortex, insula, midcingulate cortex, and thalamus. Notably, these regions were consistently recruited regardless of stimulation technique, location of induction, and participant sex. These findings suggest a highly-conserved core set of pain-related brain areas, encouraging applications as a biomarker for novel therapeutics targeting acute nociceptive pain.

Keywords: pain; neuroimaging; meta-analysis; fMRI

1. INTRODUCTION

Chronic and acute pain are global medical issues affecting at least 20% of adults globally and they are often accompanied by both comorbid psychological disorders and significant disability in daily activities (Goldberg & McGee, 2011). Given the prevalence of pain conditions, there is a need to develop tools capable of translating the subjective report of pain into an objective measure (i.e., a pain biomarker) that can be used in the development of novel treatments. Recently, neuroimaging approaches have been used to examine pain-related brain activity as a physiological biomarker of pain for treatment development (Cowen et al., 2015; Labus et al., 2015; Wager et al., 2013; Woo et al., 2017). Though the challenge of pain biomarker development is increased when chronic pain conditions are analyzed, a growing body of work examining the neural correlates of experimentally-induced, nociceptive pain in healthy volunteers has led to important insights into the mechanisms and characteristics of how the sensation of pain arises, including its cognitive, affective, and sensory dimensions that may not be reflected in self-report scales (Apkarian et al., 2005; Hofbauer et al., 2001; Robinson et al., 2013; Talbot et al., 1991; Tracey & Mantyh, 2007; Treede et al., 1999; Woo & Wager, 2016). While this work has been critical in elucidating the circuits recruited by acute nociceptive pain under a variety of experimental contexts, synthesizing these data to identify convergent patterns of pain-related brain activation can be challenging due to heterogeneity of experimental designs and samples.

To integrate findings across neuroimaging experiments, meta-analysis provides a powerful approach to quantitatively identify consistent brain regions activated during pain (Wager et al., 2009). Prior meta-analyses have identified several brain regions that are engaged under pain conditions, including the secondary somatosensory cortex (SII), insula, cingulate cortex, and thalamus. Other regions have been identified somewhat less reliably, including primary somatosensory cortex (SI), striatum, cerebellum, supplementary motor area (SMA), primary motor area (M1), periaqueductal gray (PAG), prefrontal cortex (PFC), certain areas in parietal cortices, and the parahippocampal gyrus (Apkarian et al., 2005; Duerden & Albanese, 2013; Farrell et al., 2005; Jensen et al., 2016; Lanz et al., 2011; Peyron et al.,

2000; Tanasescu et al., 2016). Subsequent meta-analyses have sought to parse this pain network further by investigating neural responses specific to different pain induction modalities, such as thermal pain (Farrell et al., 2005; Friebel et al., 2011; Jensen et al., 2016), and to different stimulation location (Duerden & Albanese, 2013; Jensen et al., 2016; Lanz et al., 2011). These meta-analyses have provided a substantial advance in our understanding of the brain's pain network. However, the significant increase in functional magnetic resonance imaging (fMRI) experiments in pain since the most recent meta-analyses (Jensen et al., 2016; Tanasescu et al., 2016) as well as an influx of articles standardizing rigorous procedures for meta-analyses (Eickhoff et al., 2016; Müller et al., 2018) suggest that an update is warranted. Furthermore, based on recent evidence of inadequate Type I error control using previously-typical statistical methods, we considered it worthwhile to revisit the topic of identifying brain regions consistently recruited by diverse pain-inducing stimuli while adhering to contemporary standards in the field (Eklund et al., 2016; Müller et al., 2018).

Accordingly, we conducted a comprehensive meta-analysis of fMRI studies of experimentally-induced pain in healthy volunteers; the analysis included findings from 222 experiments. We first sought to replicate and extend the findings from previous meta-analyses, incorporating more recent studies in this rapidly moving field. Second, we applied standards for Type I error correction to our analyses according to current standards in the field. Third, we assessed differences in pain responsiveness associated with differences in pain stimulation modality (thermal, electrical, mechanical, or chemical), location of stimulation (visceral or somatic, left or right side of body, proximal or distal extremity), and sample composition (participant sex). As described below, our results revealed highly convergent evidence for the existence of a core set of brain regions associated with acute nociceptive pain in healthy participants. This core set was present across different samples and experimental designs, encouraging its use as biomarker of acute pain that could be useful for experimental therapeutics.

2. METHODS

This is a systematic review and meta-analysis, and the methodology used adheres to PRISMA and field-standard guidelines for meta-analyses (Moher et al., 2009; Müller et al., 2018). The procedures and analyses in this meta-analysis were preregistered on PROSPERO (https://www.crd.york.ac.uk/prospero/display_record.php?RecordID=106435).

We first performed a literature search for fMRI experiments of experimentally induced pain in healthy participants using eight databases and then searched for references in reviews identified in the database. Titles and abstracts returned by this search were first evaluated for full-text screening. Full text articles were evaluated to see if they met defined inclusion criteria (see **Figure 1** for PRISMA chart detailing screening process). This screening process resulted in a total of 222 fMRI experiments from 200 articles that were included in this study. See specific details below. Coordinate data from these experiments were then extracted and analyzed using activation likelihood estimation (ALE).

2.1. Literature search

We performed a literature search for fMRI experiments of experimentally induced pain in healthy volunteers using both database searches and references cited in review articles, meta-analyses, and component studies. The final literature search took place on August 1, 2018 and was restricted to articles published from 1990 to August 1, 2018. We used 1990 as the start date of our search due to the widespread emergence of using fMRI for neuroimaging tasks such as pain starting after 1990.

2.1.1. Database search

The following standard literature databases were searched: PUBMED/MEDLINE, EMBASE, Web of Science, Cochrane Library, and PsycINFO. We used the following search terms: ("MRI" or "magnetic resonance imaging" or "fMRI" or "BOLD" or "brain mapping") AND ("pain" or "noxious" or "nociception"). We further filtered our search criteria to try to meet our inclusion criteria (section 2.2) by

including only publications that were in English, that appeared in peer-reviewed journals (e.g., not conference papers), and that included experiments conducted in humans. We supplemented our database search with the following existing fMRI data repositories: NeuroSynth (Yarkoni et al., 2011), brainspell (Toro, 2015), and BrainMap (Laird et al., 2005). In these repositories, we searched for records using the keyword "pain." Notably, we did not include grey literature in our search, as this could introduce studies that did not undergo peer review, potentially compromising the rigor of our methodology.

2.1.2. Reference search from reviews

To identify potential candidate studies from reference lists, we also screened the resulting abstracts for editorials, review articles, and meta-analyses related to pain. In editorials (i.e., non-systematic reviews), we identified titles in reference sections that seemed likely to include a pain experiment. In systematic reviews, we considered all articles that the authors identified for inclusion. If a systematic review included a meta-analysis of experimentally induced pain in healthy volunteers (e.g., Friebel et al., 2011; Duerden & Albanese, 2013; Jensen et al., 2016; Tanasescu et al., 2016), we automatically included all studies within the meta-analysis to be screened for full text.

The database search yielded a total of 7,529 articles. We additionally compiled references from existing review articles which yielded a total of 1,216 articles (total of 8,754 records). After removing duplicates, we screened a total of 4,927 abstracts.

Figure 1 about here

2.2 Inclusion Criteria

Experiments were only included in the meta-analysis if they contained a within-subject "pain > baseline" contrast (e.g., "pain > rest", "pain > innocuous stimuli" or parametric modulation of pain) that was not confounded by other experimental manipulations that could impact the acute nociceptive pain induction (e.g., treatment manipulations prior to the pain induction, such as drug infusions or placebo). If at least one experiment in an article satisfied this initial requirement, it was evaluated according to the following inclusion criteria:

1. The experiment was from a peer-reviewed journal article written in English. Prior literature has shown language restrictions to English have marginal effect on results and are dependent on the field of study (Morrison et al., 2012). We therefore did not feel this language restriction would introduce substantial bias to our results.

2. The experiment considered healthy, human participants over the age of 18. To satisfy this criterion, the study must explicitly report that all participants were healthy or free of medical or psychiatric disorders.

3. The experiment included at least 10 participants.

4. The experiment induced physical pain that was confirmed to be painful by participants. Confirmation of experienced pain could be in the form of an explicit report of the induction being painful, participant ratings of experienced pain during the scan session, or the use of a pain stimulus that was titrated to a threshold pre-determined to be painful by participants in the experiment.

5. Brain responses to induced pain were monitored using fMRI.

6. The field of view and reported results included the whole brain (i.e., region of interest analyses were excluded). This criterion was imposed so as to prevent bias towards *a priori* regions putatively thought to be involved in pain.

7. The experiment reported results in a standard stereotaxic reference space coordinate system (MNI or Talairach space).

8. Results met current statistical standards for conventional cluster identification. Specifically, we only included experiments that reported activation at a voxel-level threshold of $p < 0.001$ (uncorrected) or a corrected cluster probability of $p < 0.05$. We also excluded experiments that did not report their methods and results in sufficient detail to conclude whether they met our statistical threshold criteria.

Additionally, if experiments in articles did not report relevant results but met the inclusion criteria, we e-mailed the corresponding authors and included the experiment if data was provided. A PICOS figure of our search and eligibility criteria is included in **Supplementary Table 2**.

2.2.2. Abstract and Full Text Assessment

Two independent reviewers (AX, EBB) confirmed the inclusion or exclusion of each abstract for full text screening. Abstracts were first assessed as to whether they included a physical pain contrast in healthy volunteers and whether they measured task-based blood-oxygen-level-dependent (BOLD) responses. In this stage of screening, we only excluded abstracts that explicitly mentioned (1) having a sample size of less than 10 subjects; (2) using only a neuroimaging modality that was not fMRI, such as EEG; or (3) only including animal experiments. Note that in this stage of screening, we did not exclude any papers that involved a clinical population, used resting-state fMRI, or involved a treatment or intervention. These criteria allowed us to assess parts of seemingly irrelevant papers that may have included relevant experiments for analyses, such as including a healthy subsample (e.g., the control sample) or a task-based measure involving acute nociceptive pain (e.g., pain inductions either pre-treatment or post-resting-state). Full text articles from included abstracts were then assessed for whether they met our inclusion criteria (see section 2.2.1. Inclusion Criteria). Finally, at least two independent reviewers confirmed the decision for inclusion of articles marked for inclusion in the final analysis (AX, BL, EB). In cases of reviewer decision disagreement, a senior third reviewer (TS) evaluated the article.

2.3. Data extraction

Coordinates and information about each experiment were extracted manually by at least one author (AX or VS) and checked independently by another member of the study team (AX or VS). The following information about each paper was extracted: sample size; whether the coordinate space was MNI or Talairach; modality of pain stimulus (e.g., thermal, electrical, mechanical, or chemical); side the stimulus was induced; whether the stimulus was on the arm (not including hand), leg (not including foot),

hand, or foot; whether the pain stimulus was visceral (e.g., esophageal distension); and whether the reported activation included a non-painful control stimulus (e.g. painful > innocuous contrast).

In cases where studies contained multiple relevant pain contrast results from a single experiment, we chose to use results that were most likely to demonstrate a clear nociceptive pain-specific signal. For example, when experiments contained separate analyses based on the intensity of the pain induction (e.g., one contrast for moderate pain and another for high pain), we chose the contrast for the highest intensity of pain reported (e.g., high pain). For experiments with separate analyses based on a subjective rating of pain and based on an objective intensity, we included results based on the objective intensity rather than the subjective rating.

If multiple experimental contrasts included in a single article could be used for different sets of meta-analyses (see section 2.4.2.), we first pooled coordinates from each experiment into one set of coordinates for that particular article and treated this set of coordinates as one experiment in our primary meta-analysis (Turkeltaub et al., 2012). This approach ensured that we only used one set of coordinates per article, so that one specific article could not be weighted more heavily than others due to the presence of multiple relevant experiments (Müller et al., 2018; Turkeltaub et al., 2012). For example, for our primary meta-analysis of experimentally-induced pain, if an article contained multiple experiments using different types of pain stimulation (e.g., thermal and mechanical), we pooled the results from both types of pain stimulation together and treated the results as if they were derived from one experiment. For any additional analyses (see section 2.4.2.), we evaluated these contrasts separately(e.g., the thermal set of coordinates would be tagged as thermal pain and treated as one experiment while the mechanical set of coordinates would be tagged as mechanical pain and treated as another experiment).

2.4. Coordinate based meta-analysis

2.4.1. Activation likelihood estimation (ALE)

We conducted meta-analyses using the coordinate-based meta-analytic method activation likelihood estimation (ALE) (Turkeltaub et al., 2002) using the revised algorithm that allows for random effects inference (Eickhoff et al., 2009; Eickhoff et al., 2012; Rottschy et al., 2012). The main effect for a particular condition of interest is defined by the convergence of activation from all relevant experiments included in analyses.

Briefly, for each experiment included, ALE treats coordinates for the foci of reported clusters as the center of an uncertainty function modeled by a 3D Gaussian probability distribution. The full width at half-maximum (FWHM) of this 3D Gaussian kernel was determined by empirical data on between-subject and between-template (i.e., MNI or Talairach space coordinates) variance. Specifically, the algorithm takes into account between-subject variance by using a tighter Gaussian distribution for experiments with greater sample sizes to represent that these experiments should provide more reliable results of a true activation effect (Eickhoff et al., 2009), and it takes into account between-template differences by transforming coordinates reported in Talairach coordinates into MNI coordinates (Lancaster et al., 2007). This model then provides probabilities for all activation foci in each experiment, which were combined for each voxel, resulting in an individual modeled activation (MA) map for each experiment. By taking the union across all the MA-maps, we generated voxelwise ALE scores that describe the convergence of results at each particular location (Eickhoff et al., 2009). Note that MA-values reflect data for a single experiment while ALE-values integrate data across multiple experiments.

For ALE maps, the *p*-value was defined as the proportion of values obtained under a null distribution reflecting a random spatial association between experiments. The resulting non-parametric *p* values were subsequently thresholded using voxel height threshold of $p < 0.001$, reflecting current recommendations for best practices (Eklund et al., 2016). At this voxel height, the significance of cluster extent was estimated using 10,000 Monte-Carlo simulations; this distribution was calculated specifically

for each meta-analysis conducted (Eickhoff et al., 2012; Rottschy et al., 2012). Clusters were considered significant if they achieved a family-wise corrected significance of $p < 0.05$. Prior to display, p-values were then transformed into z scores. All results were labeled using either SPM Anatomy Toolbox v2.2 (Eickhoff et al., 2005) or Harvard-Oxford Structural Atlas (Kennedy et al., 1998) distributed by FSL. Thalamic parcellations included with SPM Anatomy Toolbox were based on the Thalamic Connectivity Atlas (Behrens et al., 2003).

2.4.1.1. Statistical contrasts

To analyze differences in convergent activation (i.e., differing convergence of results) between two different groups of experiments, we computed the voxel-wise differences between the cluster-level FWE-corrected maps derived from the individual main effect analyses (as described above). To determine the significant difference in ALE scores, we first generated a null distribution of ALE-score differences by randomly permuting the labels of all experiments, dividing them into two groups of the same sizes as the original analysis, and calculating the ALE-scores for these two randomly permuted groups for all voxels in the brain. We repeated this process 10,000 times and tested the observed differences in ALE-scores against the derived null distribution. We thresholded probability values at $p < 0.001$ and inclusively masked them by the main effects for the particular condition of interest. Finally, we applied an extent-threshold of $k > 25$ voxels. It is important to note, however, that an unequal proportion of experiments in the two groups of interest could bias the observed results. To address this concern, we conducted chi-squared tests for differences in proportion of experiments between the two groups of interest in each of our planned contrasts, and we limited our analyses to comparisons that did not significantly differ in number of experiments (at $p < 0.01$).

2.4.1.2. Conjunction Analyses

To analyze voxels where a significant effect was present in two different groups of experiments, we computed their conjunction using the conservative minimum statistic (Nichols et al., 2005). This

approach is equivalent to identifying the intersection between each of the cluster-level FWE-corrected maps of the main effects for the two groups of experiments (Caspers et al., 2010). We then applied an extent-threshold of $k > 25$ voxels to exclude smaller regions of presumably incidental overlap between the two maps of the main effects.

2.4.2. Effects of interest

We primarily focused on finding areas consistently reported to be activated in response to noxious stimuli inducing acute pain. We first assessed areas converging in activation in response to pain using all of our extracted coordinate data (with only one set of coordinates per article). However, because some of our included experiments used a contrast of "pain > rest" while others used a contrast of "pain > innocuous stimuli", we conducted secondary analyses examining the main effect of the experiments using the contrast "pain > rest" and then the experiments using "pain > innocuous stimuli." A contrast between experiments using "pain > rest" contrast and "pain > innocuous stimuli" contrast, however, was not computed due to significant differences in the proportion of experiments using the "pain > rest" contrast and the "pain > innocuous stimuli" contrast.

Next, given the heterogeneity of the different pain induction techniques used in the included experiments, we conducted additional contrast and conjunction analyses that examined the effect of different modalities and locations of pain inductions as well as the sex of the sample. The following analyses were conducted:

- To analyze the effect of pain modalities considered, we examined experiments inducing thermal pain (e.g., heat, cold), mechanical pain (e.g., pin prick, pressure, distension), electrical pain (e.g., electrical stimulation), and chemical pain (e.g., capsaicin). To explicitly compare different modalities, we conducted between-experiment contrasts comparing thermal and non-thermal experiments as well as electrical and mechanical experiments. Further analyses comparing other modalities could not be reliably conducted based on significant differences in the proportion of experiments available.

- To examine effects of the location of induced pain, we conducted three separate contrasts. First, we evaluated laterality by contrasting experiments where pain was induced on the left side versus the right side of the body. Second, we examined differences in the effect of inducing pain on the extremities at proximal (i.e., the arm or leg) versus distal (i.e., the hand or foot) locations, which have different densities of nociceptors. Third, we examined differences in brain activation for visceral (e.g., rectal distension) versus non-visceral (i.e., somatic) pain. Notably, we only included non-visceral mechanical pain, because all visceral pain inductions were mechanical.

- Finally, by comparing experiments that included *only* male or *only* female participants, we sought to evaluate sex differences in the pain response (e.g., Coen et al., 2008).

2.4.5. Post-hoc diagnostics

To address bias and heterogeneity of experiments included in our primary meta-analysis of pain, we calculated the contribution of each experiment by computing the ratio of ALE-scores of all voxels in a specific cluster with and without each experiment. Similarly, we calculated the contribution of different conditions of interest from groups of experiments (e.g., thermal, mechanical, right-sided pain, left-sided pain, etc.). These analyses provided an estimate of how the ALE-score changed when the experiment or group of experiments in question was removed (see Cieslik et al., 2016 for example). However, given the large number of experiments included in this study, undue influence of a single experiment was relatively unlikely (Eickhoff et al., 2012).

3. RESULTS

Our search, screening, and evaluation yielded a total of 222 experiments from 200 articles that met inclusion criteria as confirmed by two independent reviewers (**Figure 1**). Of these 222 experiments, we meta-analyzed 200 experiments for the main effect of induction of a reported sensation of pain.

Among these, 62 experiments used a "pain > innocuous" contrast and 134 experiments used a "pain > rest" contrast. The remaining 3 experiments examined a parametric modulation of pain.

For modality-specific analyses, we meta-analyzed 107 thermal pain experiments (inducing heat pain or cold pain) and 98 non-thermal pain experiments. The non-thermal pain experiments included 39 experiments inducing electrical pain (e.g., electric shocks), 46 inducing mechanical pain (e.g., pressure pain, distension), and 13 inducing chemical pain (e.g., capsaicin). For location-specific analyses, we meta-analyzed 92 left-sided pain experiments, 66 right-sided pain experiments, 68 experiments inducing pain in distal extremities, 85 experiments inducing pain in proximal extremities, 17 experiments inducing visceral pain, and 29 experiments inducing non-visceral (mechanical) pain. Finally, for sample composition-related analyses, we meta-analyzed 22 all-female experiments and 30 all-male experiments (**Figure 2; Table 1**).

Figure 2 about here

Table 1 about here

3.1. Main effect of stimuli inducing a sensation of pain

Meta-analysis of pain experiments from all studies (*n* = 200), which included experiments using the contrasts "pain > rest" and "pain > innocuous" as well as parametric modulation of pain, revealed significant pain-related convergence of activation in four large clusters, with peak activation magnitudes located in the right supramarginal gyrus (inferior parietal lobule, IPL), right midcingulate cortex (MCC), right precentral gyrus, and left cerebellum (**Figure 3**; **Table 2**). Further examination of these large clusters revealed activation in the bilateral thalamus, bilateral SMA, bilateral pre-SMA, bilateral putamen, bilateral caudate, bilateral brainstem, bilateral amygdala, right middle frontal gyrus, left supramarginal gyrus/IPL (insula) and left MCC. Post-hoc analysis confirmed these results were not significantly impacted by any individual experiment (see **Supplementary Table 1**).

Figure 3 about here

Table 2 about here

We next evaluated experiments reporting a "pain > rest" contrast ($n = 134$) and "pain >
innocuous" contrast ($n = 62$), as "pain > innocuous" contrasts controlled for the impact of sensorimotor
stimulation (e.g., touch). In experiments reporting a "pain > rest" contrast, we found significant activation
in seven clusters, with peak activation magnitudes located in bilateral IPL (right supramarginal gyrus and
left intraparietal sulcus), right MCC, right precentral gyrus, left insula, left thalamus, and left cerebellum
(**Figure 4A; Table 3**). Activation in these clusters also comprised of bilateral SMA, bilateral pre-SMA,
bilateral putamen, bilateral caudate, right brainstem, right insula, right middle frontal gyrus, right
amygdala, left MCC, and left precentral gyrus. In experiments using a "pain > innocuous" contrast, we
found significant activation in four clusters, with peak activation magnitudes located in bilateral insula,
right MCC, and right thalamus (**Figure 4B; Table 3**). These clusters were also comprised of the bilateral
putamen, bilateral SMA, left MCC, left thalamus, right amygdala, right precentral gyrus and right pre-
SMA. Due to statistically significant differences in number of experiments reporting these contrasts ($\chi^2(1)$
$= 27.33$, $p < 0.001$), we did not perform an explicit contrast between experiments reporting a "pain > rest"
contrast and a "pain > innocuous" contrast.

<div align="center">**Figure 4 about here**</div>

<div align="center">**Table 3 about here**</div>

3.2. Effect of stimulus modality

3.2.1. Thermal and non-thermal pain

To examine modality-specific effects of pain induction, we first compared experiments that
induced thermal pain ($n = 107$) with experiments that induced non-thermal pain ($n = 98$). Experiments
inducing thermal pain showed convergence of activation in five clusters, with peak activation magnitudes
located in right Rolandic operculum/IPL (posterior insula), right MCC, right middle frontal gyrus, right
precentral gyrus, and left cerebellum (**Figure 5A; Table 4**). Further examination of these large clusters
revealed activation in bilateral putamen, bilateral caudate, bilateral brainstem, bilateral SMA, bilateral
pre-SMA, left Rolandic operculum/IPL, left MCC, and right amygdala. Experiments inducing non-

thermal pain also showed activation in five clusters, with peak activation magnitudes located in right

Rolandic operculum, right MCC, right thalamus, right middle frontal gyrus, and left postcentral gyrus

(SII) (**Figure 5B; Table 4**). Further examination of these large clusters revealed activation in bilateral

SMA, bilateral putamen, bilateral pre-SMA, left MCC, and left thalamus. An explicit contrast between

thermal and non-thermal pain experiments revealed significantly stronger convergence of activation in

bilateral MCC for thermal experiments, and stronger convergence in the right insula and left Rolandic

operculum in non-thermal experiments (**Table 4**). Conjunction analyses revealed widespread overlap

between thermal and non-thermal pain experiments in six large clusters, with peak activation magnitudes

located in bilateral supramarginal gyrus (SII), bilateral thalamus, right MCC, and right middle frontal

gyrus (**Table 4**). These large clusters also included the bilateral putamen, bilateral SMA, left MCC, and

right amygdala.

<div align="center">

Figure 5 about here

Table 4 about here

</div>

3.2.2. Electrical, mechanical, and chemical pain

We next examined the effect of electrical (*n* = 39), mechanical (*n* = 46), and chemical (*n* = 13)

pain induction (**Figure 6** and **Figure 7**). Experiments inducing electrical stimulation to evoke pain

showed convergence of activation in five large clusters, with peak activation magnitudes located in

bilateral thalamus, right MCC, right Rolandic operculum, and left postcentral gyrus (SII) (**Figure 6A;**

Table 5). Experiments inducing mechanical pain showed convergence of activation in seven large

clusters, with peak activation magnitudes located in bilateral insula, bilateral supramarginal gyrus

(consisting of SII and IPL), bilateral thalamus, and right MCC (**Figure 6B; Table 5**). Further examination

of these large clusters associated with mechanical pain revealed activation including the bilateral putamen

and left MCC. An explicit contrast between electrical and mechanical pain experiments revealed greater

activation in the right Rolandic operculum, right thalamus, and right superior temporal gyrus in electrical

pain experiments. In no cases was greater activation seen for mechanical pain experiments (**Table 5**).

Conjunction analyses revealed widespread overlap of convergence of activation between electrical and

mechanical pain experiments in seven large clusters, with peak activation magnitudes located in bilateral insula, bilateral SII (left postcentral gyrus and right supramarginal gyrus), bilateral thalamus, and right MCC (**Table 5**).

<div align="center">**Figure 6 about here**</div>

<div align="center">**Table 5 about here**</div>

Finally, chemical pain experiments showed convergence of activation in ten clusters, with peak activation magnitudes located in ventral aspects of the brainstem, bilateral insula (with two clusters in the left insula), bilateral thalamus, left Rolandic operculum, left MCC, left SMA, and right postcentral gyrus/IPL (**Figure 7; Table 6**). Further examination of these large clusters revealed activation within the right MCC and midbrain. There were not a sufficient number of chemical pain induction comparisons to contrast chemical pain-related activation with electrical stimulation-provoked pain ($X^2(1) = 13$, $p < 0.001$), mechanical pain ($X^2(1) = 18.45$, $p < 0.001$), or thermal pain ($X^2(1) = 73.63$, $p < 0.001$).

<div align="center">**Figure 7 about here**</div>

<div align="center">**Table 6 about here**</div>

3.3. Effect of stimulus location

3.3.1. Laterality

To examine location-specific effects of nociceptive pain induction, we compared experiments that induced left-sided pain ($n = 92$) with experiments that induced right-sided pain ($n = 66$). Experiments inducing left-sided pain showed convergence of activation in six clusters, with peak activation magnitudes located in right Rolandic operculum, right MCC, right middle frontal gyrus, and right postcentral gyrus, left supramarginal gyrus, and left cerebellum (**Figure 8A; Table 7**). Further examination of these large clusters revealed activation in bilateral insula, bilateral thalamus, bilateral pre-SMA, left MCC, right amygdala, right pallidum and the brainstem. Experiments inducing right-sided pain showed convergence of activation in nine clusters, with peak activation magnitudes located in bilateral thalamus, left Rolandic operculum, right supramarginal gyrus, right MCC, right middle frontal gyrus,

right IPL, right precentral gyrus and right insula (**Figure 8B, Table 7**). Further examination of these large clusters revealed activation in bilateral putamen, bilateral SMA, bilateral pre-SMA, left MCC, left insula, and right precentral gyrus.

An explicit contrast between left- and right-sided stimulation experiments did not reveal any clusters with stronger convergence of activation in left-sided pain induction experiments but did reveal stronger convergence of activation in left Rolandic operculum (SII) in right-sided pain induction experiments (**Table 7**). Given that we did not see involvement of SI in right-sided pain induction based on these analyses (despite reports of SI involvement in pain (Bushnell, 1999)), we also separately examined unthresholded maps and found involvement of right SI, suggesting that while SI did not appear prominently in our explicit contrast, there may still be some laterality in SI that is harder to detect. SI was particularly prominent when the stimulation site was more tightly aligned across studies (e.g., left-sided arm stimulation).

Finally, conjunction analyses revealed widespread overlap of convergence of activation between left-sided and right-sided experiments in eight clusters, with peak activation magnitudes located in bilateral insula, bilateral supramarginal gyrus (consisting of IPL), bilateral thalamus, right MCC, and right middle frontal gyrus (**Table 7**). Further evaluation of these clusters revealed activation in the left MCC, right putamen, and right SMA.

<div align="center">

Figure 8 about here

Table 7 about here

</div>

3.3.2. Distal and proximal extremities

We next compared experiments inducing distal nociceptive pain in the hand or foot ($n = 68$) with experiments inducing proximal pain in the arm or leg ($n = 85$). Experiments inducing distal pain in the hand or foot also showed convergence of activation in six clusters, with peak activation magnitudes located in bilateral IPL (consisting of right Rolandic operculum and left supramarginal gyrus), bilateral thalamus, right MCC, and right middle frontal gyrus (**Figure 9A; Table 8**). Further examination of these large clusters revealed activation in bilateral insula, bilateral amygdala, bilateral pre-SMA, and right

SMA. Experiments inducing proximal pain showed convergence of activation in six clusters, with peak activation magnitudes located in right Rolandic operculum, right MCC, right middle frontal gyrus, right precentral gyrus, right post central gyrus, and left insula (**Figure 9B; Table 8**). These large clusters included the bilateral pre-SMA, bilateral subnuclei of the striatum, right insula, right SMA, and left MCC. An explicit contrast between proximal and distal stimulation experiments did not reveal differential patterns of activation, while conjunction analyses revealed widespread overlap convergence of activation in eight clusters (**Table 8**). These eight clusters included bilateral thalamus, bilateral IPL (represented by left supramarginal gyrus and right operculum), right MCC (with spread to left MCC), right middle frontal gyrus, right pallidum, and left insula.

Figure 9 about here

Table 8 about here

3.3.3. Effect of acute visceral and non-visceral mechanical nociceptive pain

We compared experiments inducing visceral pain (e.g., distension in the rectum, esophagus, or stomach; $n = 17$) with experiments inducing non-visceral mechanical pain ($n = 29$). Experiments inducing visceral pain showed convergence of activation in five clusters, with peak activation magnitudes located in right supramarginal gyrus, right Rolandic operculum, left putamen, left thalamus, and right MCC (**Figure 10A; Table 9**). Non-visceral mechanical pain experiments showed convergence of activation in ten clusters, with peak activation magnitudes located in bilateral supramarginal gyrus (SII), bilateral insula (with two clusters in the right insula), bilateral thalamus, right Rolandic operculum, right caudate nucleus, and right MCC (**Figure 10B; Table 9**). An explicit contrast between visceral and non-visceral mechanical pain experiments did not reveal differential activation, while conjunction analyses revealed overlap of convergence in two clusters—the right supramarginal gyrus and the left thalamus (**Table 9**).

Figure 10 about here

Table 9 about here

3.4. Effect of sex

We examined sex differences in nociceptive pain responses by comparing experiments with an all-female sample ($n = 22$) to those with an all-male sample ($n = 30$). Experiments with an all-female sample showed convergence of activation in five clusters, with peak activation magnitudes located in bilateral IPL (represented by left superior temporal gyrus and right supramarginal gyrus) and bilateral insula (with two clusters in the left insula; see **Figure 11A** and **Table 10**). Experiments with an all-male sample showed convergence of activation in eight clusters, with peak activation magnitudes located in bilateral insula, bilateral thalamus, right MCC (spreading into the left hemisphere), right temporal pole (spreading into the precentral gyrus), right middle frontal gyrus and right Rolandic operculum (**Figure 11B; Table 10**). An explicit contrast between males and females did not reveal differential activation (**Table 10**), while conjunction analyses revealed overlap in three clusters—bilateral insula and left supramarginal gyrus/IPL (**Table 10**).

Figure 11 about here

Table 10 about here

4. DISCUSSION

We conducted what is to our knowledge the largest fMRI meta-analysis of experimentally induced pain in healthy volunteers to date, applying rigorous type I error control and stringent inclusion criteria. We first synthesized results across 200 experiments, revealing a network of regions consistently activated by acute nociceptive pain in healthy participants. We further interrogated the modulation of stimulation modality, stimulation location, and sex and found a largely consistent pattern of activation in a core set of brain regions, irrespective of the specific experimental paradigm. These regions include the thalamus, MCC, SII, insula, as well as portions of the supramarginal gyrus/IPL and Rolandic operculum. In a smaller number of analyses, we observed involvement of the lateral PFC, precentral gyrus, SMA, pre-SMA, cerebellum, the brainstem, basal ganglia (putamen, caudate, and palladium), amygdala, and postcentral gyrus (SI**; Figure 12**).

Figure 12 about here

Our primary meta-analysis revealed a "pain network" of convergent activation across 200 experiments that was largely consistent with the findings of other similar recent meta-analyses (Friebel et al., 2011; Duerden & Albanese, 2013; Jensen et al., 2016; Tanasescu et al., 2016). As in prior meta-analyses, we found evidence of pain-related activation of bilateral thalamus, cingulate cortex, insula, SII, motor areas, and right middle frontal gyrus (Friebel et al., 2011; Duerden & Albanese, 2013; Jensen et al., 2016; Tanasescu et al., 2016). However, a subset of brain areas identified here are less consistently reported in earlier work, including the basal ganglia (putamen) (Duerden & Albanese, 2013; Jensen et al., 2016; Tanasescu et al., 2016), the amygdala (Jensen et al., 2016; Tanasescu et al., 2016), and the brainstem (Tanasescu et al., 2016). Notably, previous meta-analyses have reported activation in SI and the right cerebellum (Duerden & Albanese, 2013; Jensen et al., 2016; Tanasescu et al., 2016), which were not found here. To the degree that there is variation between our results and prior meta-analyses, these may in part reflect differences in the sample and methodological approach. Specifically, we considered the largest sample to date of studies which passed rigorous inclusion criteria (e.g., at least 10 participants,

cluster $p < 0.001$ or FWE-corrected). Additionally, in line with current recommendations (e.g., Eklund et al., 2016 and Eickhoff et al., 2016), we applied a more stringent statistical correction to our results than prior meta-analyses.

We found qualitative evidence for more activation of SII, insula, MCC, thalamus, SMA, pre-SMA, MCC, and right amygdala in experiments using an innocuous control compared to those that used a resting baseline. In contrast, experiments using a resting baseline had significant convergence of activation in right lateral PFC, right precentral gyrus, left cerebellum, and bilateral subnuclei of the basal ganglia (putamen, caudate) that were not identified in our analysis of experiments using an innocuous control. These findings suggest that these areas may not be response to pain per se, but rather a general response to sensory stimulation. While these qualitative findings are interesting, we did not conduct a direct, quantitative comparison of studies using a sensorimotor control and a resting baseline due to differences in the number of experiments using these approaches. Specifically, there was a significantly greater number of experiments using a resting baseline than experiments using an innocuous control. As such, it is difficult to conclude whether observed differences are in part driven by differences in the number of experiments included. Nevertheless, the qualitative differences between these two contrasts may still be meaningful and ultimately expected, as contrasts against a resting baseline will also reflect sensorimotor processing. To better separate the pain response from non-specific sensory responses, studies are needed that explicitly compare these two baseline conditions.

To further interrogate variability in the pain response that may be sensitive to differences in other experimental design considerations, we conducted a set of sub-analyses that investigate the effects of stimulation modality, stimulation location, and sex of sample. These analyses revealed a core set of brain areas that were consistently and robustly activated by pain regardless of experimental design, as well as regions that are more variably activated by pain across experiments. We discuss these areas in detail below**.**

4.1. Core regions consistently activated by pain

The thalamus, SII, MCC, and insula were the most robustly activated brain areas across all experimental paradigms. This core set of brain regions has been implicated in sensory-discriminative and affective-motivational aspects of pain (Tracey & Mantyh, 2007; Treede et al., 1999). The thalamus processes and transmits nociceptive information between the spinal cord and cortex (Yen & Lu, 2013; Ab Aziz & Ahmad, 2006) while the SII may reflect higher-order sensory representation, especially information from sensory stimuli requiring more attention (Chen et al., 2008; Ferretti et al., 2003). Here, we found consistent activation of SII even in experiments that include a specific sensorimotor control condition, supporting a role for SII that goes beyond basic sensory processing, and concords with previous pain imaging studies demonstrating bilateral SII activation (Mazzola et al., 2006).

The MCC is strongly implicated in the affective-motivational components of pain, especially pain response selection (Medford & Critchley, 2010; Shackman et al., 2011; Vogt, 2005, 2016; Vogt, Berger, & Derbyshire, 2003), and has been reported in previous meta-analyses of pain (Farrell et al., 2005; Friebel et al., 2011; Peyron et al., 2000; Tillisch et al., 2011). While other meta-analyses and reviews have highlighted involvement of the anterior cingulate (ACC) in pain (Apkarian et al., 2005; Duerden & Albanese, 2013; Jensen et al., 2016; Lanz et al., 2011; Peyron et al., 2000), it should be noted that our MCC results overlap with what has sometimes been labeled as ACC. Moreover, the convergence of mid-cingulate activation associated with pain (rather than anterior regions of the cingulate) support delineations of the cingulate cortex, with the middle cingulate being more involved in pain compared to anterior regions (Shackman et al., 2011; Vogt et al., 2016).

The insula is thought to play a more indirect role in pain perception by integrating exteroceptive and interoceptive information into awareness and subjective feelings towards salient information (Craig et al. 2000; Isnard et al., 2011; Craig, 2009; Kurth et al., 2010), especially via its functional connections to the cingulate cortex (Taylor et al., 2009). The posterior portion of the insula in particular has been implicated in processing bodily information (e.g., painful sensations, somatosensory stimulation, interoception) while the anterior insula may be more involved in salience detection (Craig, 2009; Kurth et al., 2010; Menon & Uddin, 2010). As such, our meta-analytic findings of widespread insula activation

associated with pain are consistent with involvement of both anterior and posterior insula involved in acute nociceptive pain (Kurth et al., 2010).

4.2. Regions less consistently activated by pain

In addition to the core set of pain-sensitive brain areas described above, a broader set of pain-associated regions were somewhat less consistently recruited, emerging only in specific cases. These regions include the lateral PFC, M1, SMA (and portions of the pre-SMA), cerebellum, brainstem, SI, basal ganglia (putamen, caudate, and pallidum), and the amygdala. These areas have been previously reported to have less consistent and possibly more nuanced involvement in responses to pain (Apkarian et al., 2005; Duerden & Albanese, 2013; Farrell et al., 2005; Friebel et al., 2011; Lanz et al., 2011; Peyron et al., 2000; Tillisch et al., 2011). Lateral PFC (represented by the middle frontal gyrus) is typically associated with executive control and attention (Bingel & Tracey, 2008; Lorenz et al., 2003; Wiech et al., 2008), while MI, SMA, and cerebellum have typically been associated with execution of motor responses to avoid pain (Apkarian et al., 2005; Peyron et al., 2000; Moulton et al., 2010). The brainstem receives nociceptive input from the spinal cord and trigeminal nucleus and is also involved in the descending modulation of pain (Basbaum & Fields, 1978; Stamford, 1995), while basal ganglia involvement in pain may reflect modulation of multisensory integration related to pain (Borsook et al., 2010; Chudler & Dong, 1995). We observed convergent amygdala activation in four main effects analyses; the amygdala receives dense projections from nociresponsive neurons in the lateral parabrachial nucleus (Jasmin et al., 1997), has been associated with affective modulation of pain and salience detection, and has been reported in both experimental pain and chronic pain experiments (Simons et al., 2014; Borsook et al., 2013; Fernando et al., 2013).

Finally, we did not find consistent involvement of SI in the experimentally-induced pain despite its prior inclusion in a putative "pain matrix" (Iannetti & Mouraux, 2010; Legrain et al., 2011). However, we were able to detect SI involvement in pain in our meta-analyses of left-sided pain and of pain induced in proximal extremities. This less consistent involvement of SI is not surprising; previous reviews have

similarly reported less consistent activation of SI in response to painful stimulation compared to other areas (Bushnell et al., 1999; Friebel et al., 2011; Lanz et al., 2011; Peyron et al., 2000). Though SI is known to be critical for the sensory-discriminative aspect of pain (Bushnell et al., 1999; Duerden & Albanese, 2013; Friebel et al., 2011; Peyron et al., 2000), the inconsistency of SI's specific involvement in pain processing may stem from variable anatomy of SI in individual participants and, more importantly, the precise, localized somatotopic organization of SI (Bushnell et al., 1999). Our results cohere with this interpretation, as SI appeared only in analyses where there was less variability in the stimulation site (e.g., left-sided pain). Considering the highly somatotopic organization of SI, meta-analyses may need to focus on experiments of pain that target precisely the same physical locations of pain induction in order to reliably detect SI activation.

4.3. Differences between experimental pain paradigms

While the predominant pattern of results suggests consistent activation in a core set of regions accompanied by less consistent activation in other areas, we also observed important differences among paradigms. Specifically, we found stronger convergence of activation in right MCC in thermal pain experiments compared to non-thermal pain experiments – a finding consistent with earlier work by Friebel et al. (2011). Given the role of MCC in affective-motivational components of pain (Tracey et al., 2007), our results suggest that thermal experiments may be more affectively-valanced than non-thermal experiments. Notably, our findings indicate a more restricted extent of differences between thermal and non-thermal stimulation than that reported in an earlier meta-analysis by Friebel and colleagues (2011). These differences may be explained in part by the more stringent inclusion criteria and statistical threshold used in our meta-analysis.

We also found differences in the pain response to electrical stimulation compared to mechanical stimulation. Electrical experiments showed stronger convergence of activation in right Rolandic operculum, right thalamus, and right superior temporal gyrus. In contrast, mechanical experiments did not produce greater convergence of activation. These differences, however, are better characterized by a

differing extent of convergence of activation rather than different brain areas being recruited. Indeed, we find more widespread significant conjunction of activation between these stimulus modalities than significant differences. Nevertheless, our findings may suggest more robust activation of pain-sensitive brain areas in response to electrical stimulation rather than mechanical stimulation.

The meta-analyses focused on stimulation location primarily revealed a laterality effect. Right-sided pain experiments showed stronger convergence of activation in left SII. However, left-sided pain experiments did not show stronger convergence of activation in right SII. There are currently mixed findings over the extent of contralateral bias in somatotopic encoding in SII (Bingel et al., 2004; Johansen-Berg et al., 2000; Maldjian et al., 1999; Ruben et al., 2001). The stronger convergence of activation in SII may lend support for some contralateral bias in somatotopic encoding of laterality, though further studies are needed to address this more directly. Interestingly, we did not observe differences in our other location-related sub-analyses that focused on proximal versus distal pain and visceral versus non-visceral pain. These findings may suggest that central processing of pain is largely robust to differences in location of pain stimulation.

4.4. Limitations and future directions

Several limitations should be noted. As mentioned above, our findings delineate a convergent set of brain regions recruited across different experimental paradigms of pain, but an explicit meta-analysis of experiments using within-subject contrasts would better elucidate true differences in brain activation between paradigms. Given the limited number experiments that did explicitly test these differences within-subject, there is great potential for future experiments and meta-analyses to examine differences between experimental paradigms more conclusively. Similarly, because our meta-analysis relied on the published results of past articles, publication bias towards selectively publishing significant findings (and, consequently, difficulty in accounting for unpublished results) may have limited our findings (Müller et al., 2018). Additionally, it is possible that the wide range of image acquisition parameters in the experiments included may have limited the likelihood of observing some types of effects, particularly if

detection sensitivity is related to acquisition parameters (e.g., brainstem, as mentioned in Sclocco et al., 2018). While we cannot exclude the possibility of other regions being more robustly involved in or associated with pain, open sharing of imaging data may allow for better detection of these regions using image-based meta-analytic methods (Salimi-Khorshidi et al., 2009) rather than solely using coordinate-based methods.

5. CONCLUSION

Convergent results demonstrate that SII, insula, MCC, and thalamus are consistently recruited by acute nociceptive stimuli in healthy subjects across many different experimental paradigms. In contrast, lateral PFC, M1, SMA, cerebellum, brainstem, SI, and the amygdala appear from the current meta-analysis to be more variably involved. Notably, we did not find strong evidence for preferential involvement of any of these brain areas in one specific experimental stimulus paradigm over another. Taken together, these findings suggest that acute pain induction in healthy volunteers consistently recruits a core brain network. If this network overlaps with that which is involved in clinical pain, this "pain biomarker" may offer translational opportunities for fMRI in drug development and in clinical trials.

Running title: Pain fMRI Meta-analysis

REFERENCES

Ab Aziz, C. B., & Ahmad, A. H. (2006). The Role of the Thalamus in Modulating Pain. *The Malaysian Journal of Medical Sciences : MJMS*, *13*(2), 11–18.

Apkarian, A. V., Bushnell, M. C., Treede, R.-D., & Zubieta, J.-K. (2005). Human brain mechanisms of pain perception and regulation in health and disease. *European Journal of Pain*, *9*(4), 463–463. https://doi.org/10.1016/j.ejpain.2004.11.001

Basbaum, A. I., & Fields, H. L. (1978). Endogenous pain control mechanisms: Review and hypothesis. *Annals of Neurology*, *4*(5), 451–462. https://doi.org/10.1002/ana.410040511

Behrens, T. E. J., Johansen-Berg, H., Woolrich, M. W., Smith, S. M., Wheeler-Kingshott, C. A. M., Boulby, P. A., … Matthews, P. M. (2003). Non-invasive mapping of connections between human thalamus and cortex using diffusion imaging. *NATURE NEUROSCIENCE*, *6*(7), 8.

Bingel, U., Lorenz, J., Glauche, V., Knab, R., Gläscher, J., Weiller, C., Büchel, C. (2004). Somatotopic Organization of human somatosensory cortices for pain: a single trial fMRI study. *NeuroImage*, *23*(1), 224-232. https://doi.org/10.1016/j.neuroimage.2004.05.021

Bingel, U., & Tracey, I. (2008). Imaging CNS Modulation of Pain in Humans. *Physiology*, *23*(6), 371–380. https://doi.org/10.1152/physiol.00024.2008

Borsook, D., Upadhyay, J., Chudler, E. H., & Becerra, L. (2010). *A key role of the basal ganglia in pain and analgesia - insights gained through human functional imaging*. 17.

Bushnell, M. C., Duncan, G. H., Hofbauer, R. K., Ha, B., Chen, J.-I., & Carrier, B. (1999). Pain perception: Is there a role for primary somatosensory cortex? *Proceedings of the National Academy of Sciences*, *96*(14), 7705–7709. https://doi.org/10.1073/pnas.96.14.7705

Caspers, S., Zilles, K., Laird, A. R., & Eickhoff, S. B. (2010). ALE meta-analysis of action observation and imitation in the human brain. *NeuroImage*, *50*(3), 1148–1167. https://doi.org/10.1016/j.neuroimage.2009.12.112

Chen, T. L., Babiloni, C., Ferretti, A., Perrucci, M. G., Romani, G. L., Rossini, P. M., … Del Gratta, C.
(2008). Human secondary somatosensory cortex is involved in the processing of somatosensory
rare stimuli: An fMRI study. *NeuroImage*, *40*(4), 1765–1771.
https://doi.org/10.1016/j.neuroimage.2008.01.020

Chudler, E. H., & Dong, W. K. (1995). The role of the basal ganglia in nociception and pain: *Pain*, *60*(1),
3–38. https://doi.org/10.1016/0304-3959(94)00172-B

Cieslik, E. C., Seidler, I., Laird, A. R., Fox, P. T., & Eickhoff, S. B. (2016). Different involvement of
subregions within dorsal premotor and medial frontal cortex for pro- and antisaccades.
Neuroscience & Biobehavioral Reviews, *68*, 256–269.
https://doi.org/10.1016/j.neubiorev.2016.05.012

Cowen, R., Stasiowska, M. K., Laycock, H., & Bantel, C. (2015). Assessing pain objectively: the use of
physiological markers. *Anaesthesia*, *70*(7), 828–847. https://doi.org/10.1111/anae.13018

Craig, A. D. (2009). How do you feel--now? The anterior insula and human awareness. *Nature Reviews.
Neuroscience*, *10*(1), 59–70. https://doi.org/10.1038/nrn2555

Craig, A. D., Chen, K., Bandy, D., & Reiman, E. M. (2000). Thermosensory activation of insular cortex.
Nature Neuroscience, *3*(2), 184–190. https://doi.org/10.1038/72131

Duerden, E. G., & Albanese, M.C. (2013). Localization of pain-related brain activation: A meta-analysis
of neuroimaging data. *Human Brain Mapping*, *34*(1), 109–149.
https://doi.org/10.1002/hbm.21416

Eickhoff, S. B., Stephan, K. E., Mohlberg, H., Grefkes, C., Fink, G. R., Amunts, K., & Zilles, K. (2005).
A new SPM toolbox for combining probabilistic cytoarchitectonic maps and functional imaging
data. *NeuroImage*, *25*(4), 1325–1335. https://doi.org/10.1016/j.neuroimage.2004.12.034

Eickhoff, S. B., Laird, A. R., Grefkes, C., Wang, L. E., Zilles, K., & Fox, P. T. (2009). Coordinate-based
activation likelihood estimation meta-analysis of neuroimaging data: A random-effects approach
based on empirical estimates of spatial uncertainty. *Human Brain Mapping*, *30*(9), 2907–2926.
https://doi.org/10.1002/hbm.20718

Eickhoff, S. B., Bzdok, D., Laird, A. R., Kurth, F., & Fox, P. T. (2012). Activation likelihood estimation

      meta-analysis revisited. *NeuroImage*, *59*(3), 2349–2361.

      https://doi.org/10.1016/j.neuroimage.2011.09.017

Eickhoff, S. B., Nichols, T. E., Laird, A. R., Hoffstaedter, F., Amunts, K., Fox, P. T., … Eickhoff, C. R.

      (2016). Behavior, sensitivity, and power of activation likelihood estimation characterized by

      massive empirical simulation. *NeuroImage*, *137*, 70–85.

      https://doi.org/10.1016/j.neuroimage.2016.04.072

Eklund, A., Nichols, T., & Knutsson, H. (2016). Can parametric statistical methods be trusted for fMRI

      based group studies? *Proceedings of the National Academy of Sciences*, *113*(28), 7900–7905.

      https://doi.org/10.1073/pnas.1602413113

Farrell, M. J., Laird, A. R., & Egan, G. F. (2005). Brain activity associated with painfully hot stimuli

      applied to the upper limb: A meta-analysis. *Human Brain Mapping*, *25*(1), 129–139.

      https://doi.org/10.1002/hbm.20125

Ferretti, A., Babiloni, C., Gratta, C. D., Caulo, M., Tartaro, A., Bonomo, L., … Romani, G. L. (2003).

      Functional topography of the secondary somatosensory cortex for nonpainful and painful stimuli:

      an fMRI study. *NeuroImage*, *20*(3), 1625–1638.

      https://doi.org/10.1016/j.neuroimage.2003.07.004

Fernando, A. B., Murray, J. E., & Milton, A. L. (2013). The amygdala: Securing pleasure and

      avoiding pain. *Frontiers in Behavioral Neuroscience,7*. doi:10.3389/fnbeh.2013.00190\

Friebel, U., Eickhoff, S. B., & Lotze, M. (2011). Coordinate-based meta-analysis of experimentally

      induced and chronic persistent neuropathic pain. *NeuroImage*, *58*(4), 1070–1080.

      https://doi.org/10.1016/j.neuroimage.2011.07.022

Goldberg, D. S., & McGee, S. J. (2011). Pain as a global public health priority. *BMC Public Health*,

      11(1), 770. https://doi.org/10.1186/1471-2458-11-770

Hofbauer, R. K., Rainville, P., Duncan, G. H., & Bushnell, M. C. (2001). Cortical Representation of the

Sensory Dimension of Pain. *Journal of Neurophysiology*, *86*(1), 402–411.

https://doi.org/10.1152/jn.2001.86.1.402

Hu, L., & Iannetti, G. D. (2016). Painful Issues in Pain Prediction. *Trends in Neurosciences*, *39*(4), 212–220. https://doi.org/10.1016/j.tins.2016.01.004

Iannetti, G. D., & Mouraux, A. (2010). From the neuromatrix to the pain matrix (and back). *Experimental Brain Research*, *205*(1), 1–12. https://doi.org/10.1007/s00221-010-2340-1

Isnard, J., Magnin, M., Jung, J., Mauguière, F., & Garcia-Larrea, L. (2011). Does the insula tell our brain that we are in pain?: *Pain*, *152*(4), 946–951. https://doi.org/10.1016/j.pain.2010.12.025

Jasmin, L., Burkey, A. R., Card, J. P., & Basbaum, A. I. (1997). Transneuronal Labeling of a Nociceptive Pathway, the Spino-(Trigemino-)Parabrachio-Amygdaloid, in the Rat. *The Journal of Neuroscience*, *17*(10), 3751–3765. https://doi.org/10.1523/JNEUROSCI.17-10-03751.1997

Jensen, K. B., Regenbogen, C., Ohse, M. C., Frasnelli, J., Freiherr, J., & Lundström, J. N. (2016). Brain activations during pain: a neuroimaging meta-analysis of patients with pain and healthy controls. *PAIN*, *157*(6), 1279–1286. https://doi.org/10.1097/j.pain.0000000000000517

Johansen-Berg, H., Christensen, V., Woolrich, M., Matthews, P.M. (2000). Attention to touch modulates activity in both primary and secondary somatosensory areas. *NeuroReport, 11*(6), 1237-1241.

Kennedy, D. N., Lange, N., Makris, N., Bates, J., Meyer, J., & Caviness, V. S. (1998). Gyri of the human neocortex: an MRI-based analysis of volume and variance. *Cerebral Cortex (New York, N.Y.: 1991)*, *8*(4), 372–384. https://doi.org/10.1093/cercor/8.4.372

Kurth, F., Zilles, K., Fox, P. T., Laird, A. R., & Eickhoff, S. B. (2010). A link between the systems: functional differentiation and integration within the human insula revealed by meta-analysis. *Brain Structure and Function*, *214*(5–6), 519–534. https://doi.org/10.1007/s00429-010-0255-z

Labus, J. S., Van Horn, J. D., Gupta, A., Alaverdyan, M., Torgerson, C., Ashe-McNalley, C., … Mayer, E. A. (2015). Multivariate morphological brain signatures predict patients with chronic abdominal pain from healthy control subjects. *Pain*. https://doi.org/10.1097/j.pain.0000000000000196

Laird A.R, Lancaster J.L., Fox P.T. (2005). BrainMap: The social evolution of a functional neuroimaging

database. *Neuroinformatics, 3*, 65-78.

Lancaster, J. L., Tordesillas-Gutiérrez, D., Martinez, M., Salinas, F., Evans, A., Zilles, K., . . .

Fox, P. T. (2007). Bias between MNI and Talairach coordinates analyzed using the

ICBM-152 brain template. *Human Brain Mapping,28*(11), 1194-1205.

doi:10.1002/hbm.20345

Lanz, S., Seifert, F., & Maihöfner, C. (2011). Brain activity associated with pain, hyperalgesia and

allodynia: an ALE meta-analysis. *Journal of Neural Transmission*, *118*(8), 1139–1154.

https://doi.org/10.1007/s00702-011-0606-9

Legrain, V., Iannetti, G. D., Plaghki, L., & Mouraux, A. (2011). The pain matrix reloaded. *Progress in

Neurobiology*, *93*(1), 111–124. https://doi.org/10.1016/j.pneurobio.2010.10.005

Letzen, J. E., Boissoneault, J., Sevel, L. S., & Robinson, M. E. (2016). Test-retest reliability of pain-

related functional brain connectivity compared to pain self-report. *Pain*, *157*(3), 546–551.

https://doi.org/10.1097/j.pain.0000000000000356

Lorenz, J., Minoshima, S., & Casey, K. L. (2003). Keeping pain out of mind: the role of the dorsolateral

prefrontal cortex in pain modulation. *Brain*, *126*(5), 1079–1091.

https://doi.org/10.1093/brain/awg102

Maldijian, J.A., Gottschalk, A., Patel, R.S., Pincus, D., Detre, J.A., Alsop, D.C. (1999). Mapping of the

secondary somatosensory cortex activation induced by vibrational stimulation: an fMRI study.

Brain Research, 824(2), 291-295. https://doi.org/10.1016/S0006-8993(99)01126-9

Mazzola, L., Isnard, J., & Mauguière, F. (2006). Somatosensory and Pain Responses to Stimulation of the

Second Somatosensory Area (SII) in Humans. A Comparison with SI and Insular Responses.

Cerebral Cortex, *16*(7), 960–968. https://doi.org/10.1093/cercor/bhj038

Medford, N., & Critchley, H. D. (2010). Conjoint activity of anterior insular and anterior cingulate cortex:

awareness and response. *Brain Structure and Function*, *214*(5–6), 535–549.

https://doi.org/10.1007/s00429-010-0265-x

Menon, V., & Uddin, L. Q. (2010). Saliency, switching, attention and control: a network model of insula function. *Brain Structure and Function*, *214*(5), 655–667. https://doi.org/10.1007/s00429-010-0262-0

Moher, D., Liberati, A., Tetzlaff, J., Altman, D. G., & Group, T. P. (2009). Preferred Reporting Items for Systematic Reviews and Meta-Analyses: The PRISMA Statement. *PLOS Medicine*, *6*(7), e1000097. https://doi.org/10.1371/journal.pmed.1000097

Morrison, A., Polisena, J., Husereau, D., Moulton, K., Clark, M., Fiander, M., Mierzwinski-Urban, M., Clifford, T., Hutton, B., and Rabb, D., The effect of English-language restriction on systematic review-based meta-analyses: a systematic review of empirical studies. Int. J. Technol. Assess. Health Care, 28, 138–144 (2012).

Moulton, E. A., Schmahmann, J. D., Becerra, L., & Borsook, D. (2010). The cerebellum and pain: passive integrator or active participator? *Brain Research Reviews*, *65*(1), 14–27. https://doi.org/10.1016/j.brainresrev.2010.05.005

Müller, V. I., Cieslik, E. C., Laird, A. R., Fox, P. T., Radua, J., Mataix-Cols, D., … Eickhoff, S. B. (2018). Ten simple rules for neuroimaging meta-analysis. *Neuroscience & Biobehavioral Reviews*, *84*, 151–161. https://doi.org/10.1016/j.neubiorev.2017.11.012

Nichols, T., Brett, M., Andersson, J., Wager, T., & Poline, J.-B. (2005). Valid conjunction inference with the minimum statistic. *NeuroImage*, *25*(3), 653–660. https://doi.org/10.1016/j.neuroimage.2004.12.005

Peyron, R., Laurent, B., & García-Larrea, L. (2000). Functional imaging of brain responses to pain. A review and meta-analysis (2000). *Neurophysiologie Clinique/Clinical Neurophysiology*, *30*(5), 263–288. https://doi.org/10.1016/S0987-7053(00)00227-6

Robinson, M. E., Staud, R., & Price, D. D. (2013). Pain Measurement and Brain Activity: Will Neuroimages Replace Pain Ratings? *The Journal of Pain*, *14*(4), 323–327. https://doi.org/10.1016/j.jpain.2012.05.007

Rottschy, C., Langner, R., Dogan, I., Reetz, K., Laird, A. R., Schulz, J. B., … Eickhoff, S. B. (2012).

Modelling neural correlates of working memory: A coordinate-based meta-analysis. *NeuroImage*, *60*(1), 830–846. https://doi.org/10.1016/j.neuroimage.2011.11.050

Ruben, J., Schwiemann, J., Deuchert, M., Meyer, R., Krause, T., Curio, G., Villringer, K., Kurth, R., Villringer, A. (2001). Somatotopic organization of Human Secondary Somatosensory Cortex. *Cerebral Cortex, 11*(5), 462-473. https://doi.org/10.1093/cercor/11.5.463

Salimi-Khorshidi, G., Smith, S. M., Keltner, J. R., Wager, T. D., & Nichols, T. E. (2009). Meta-analysis of neuroimaging data: A comparison of image-based and coordinate-based pooling of studies. *NeuroImage*, *45*(3), 810–823. https://doi.org/10.1016/j.neuroimage.2008.12.039

Sclocco, R., Beissner, F., Bianciardi, M., Polimeni, J. R., & Napadow, V. (2018). Challenges and opportunities for brainstem neuroimaging with ultrahigh field MRI. *NeuroImage*, *168*, 412–426. https://doi.org/10.1016/j.neuroimage.2017.02.052

Shackman, A. J., Salomons, T. V., Slagter, H. A., Fox, A. S., Winter, J. J., & Davidson, R. J. (2011). The integration of negative affect, pain and cognitive control in the cingulate cortex. *Nature Reviews Neuroscience*, *12*(3), 154–167. https://doi.org/10.1038/nrn2994

Simons, L. E., Moulton, E. A., Linnman, C., Carpino, E., Becerra, L., & Borsook, D. (2014). The human amygdala and pain: evidence from neuroimaging. *Human Brain Mapping*, *35*(2), 527–538. https://doi.org/10.1002/hbm.22199

Stamford, J. A. (1995). Descending control of pain. *British Journal of Anaesthesia*, *75*(2), 217–227. https://doi.org/10.1093/bja/75.2.217

Taylor, K. S., Seminowicz, D. A., & Davis, K. D. (2009). Two systems of resting state connectivity between the insula and cingulate cortex. *Human Brain Mapping*, *30*(9), 2731–2745. https://doi.org/10.1002/hbm.20705

Talbot, J., Marrett, S., Evans, A., Meyer, E., Bushnell, M., & Duncan, G. (1991). Multiple representations of pain in human cerebral cortex. *Science*, *251*(4999), 1355–1358. https://doi.org/10.1126/science.2003220

Tanasescu, R., Cottam, W. J., Condon, L., Tench, C. R., & Auer, D. P. (2016). Functional reorganisation

in chronic pain and neural correlates of pain sensitisation: A coordinate based meta-analysis of 266 cutaneous pain fMRI studies. *Neuroscience & Biobehavioral Reviews*, *68*, 120–133. https://doi.org/10.1016/j.neubiorev.2016.04.001

Tillisch, K., Mayer, E. A., & Labus, J. S. (2011). Quantitative Meta-analysis Identifies Brain Regions Activated During Rectal Distension in Irritable Bowel Syndrome. *Gastroenterology*, *140*(1), 91–100. https://doi.org/10.1053/j.gastro.2010.07.053

Toro, R. (2015). Brainspell. [http://brainspell.org]

Tracey, I., & Mantyh, P. W. (2007). The Cerebral Signature for Pain Perception and Its Modulation. *Neuron*, *55*(3), 377–391. https://doi.org/10.1016/j.neuron.2007.07.012

Treede, R.-D., Kenshalo, D. R., Gracely, R. H., & Jones, A. K. P. (1999). The cortical representation of pain. *PAIN*, *79*(2), 105–111. https://doi.org/10.1016/S0304-3959(98)00184-5

Turkeltaub, P. E., Eden, G. F., Jones, K. M., & Zeffiro, T. A. (2002). Meta-Analysis of the Functional Neuroanatomy of Single-Word Reading: Method and Validation. *NeuroImage*, *16*(3, Part A), 765–780. https://doi.org/10.1006/nimg.2002.1131

Turkeltaub, P. E., Eickhoff, S. B., Laird, A. R., Fox, M., Wiener, M., & Fox, P. (2012). Minimizing within-experiment and within-group effects in activation likelihood estimation meta-analyses. *Human Brain Mapping*, *33*(1), 1–13. https://doi.org/10.1002/hbm.21186

Vogt, B. A. (2005). Pain and emotion interactions in subregions of the cingulate gyrus. *Nature Reviews Neuroscience*, *6*(7), 533–544. https://doi.org/10.1038/nrn1704

Vogt, B. A. (2016). Midcingulate cortex: Structure, connections, homologies, functions and diseases. *Journal of Chemical Neuroanatomy*, *74*, 28–46. https://doi.org/10.1016/j.jchemneu.2016.01.010

Vogt, B. A., Berger, G. R., & Derbyshire, S. W. G. (2003). Structural and functional dichotomy of human midcingulate cortex. *European Journal of Neuroscience*, *18*(11), 3134–3144. https://doi.org/10.1111/j.1460-9568.2003.03034.x

Wager, T. D., Lindquist, M. A., Nichols, T. E., Kober, H., & Van Snellenberg, J. X. (2009). Evaluating the consistency and specificity of neuroimaging data using meta-analysis. *NeuroImage*, *45*(1,

Supplement 1), S210–S221. https://doi.org/10.1016/j.neuroimage.2008.10.061

Wager, T. D., Atlas, L. Y., Lindquist, M. A., Roy, M., Woo, C.-W., & Kross, E. (2013). An fMRI-Based Neurologic Signature of Physical Pain. *New England Journal of Medicine*. https://doi.org/10.1056/NEJMoa1204471

Wiech, K., Ploner, M., & Tracey, I. (2008). Neurocognitive aspects of pain perception. *Trends in Cognitive Sciences*, *12*(8), 306–313. https://doi.org/10.1016/j.tics.2008.05.005

Woo, C.-W., Chang, L. J., Lindquist, M. A., & Wager, T. D. (2017). Building better biomarkers: brain models in translational neuroimaging. *Nature Neuroscience*, *20*(3), 365–377. https://doi.org/10.1038/nn.4478

Woo, C.-W., & Wager, T. D. (2016). What reliability can and cannot tell us about pain report and pain neuroimaging: *PAIN*, *157*(3), 511–513. https://doi.org/10.1097/j.pain.0000000000000442

Yarkoni, T., Poldrack, R. A., Nichols, T. E., Van Essen, D. C., & Wager, T. D. (2011). Large-scale automated synthesis of human functional neuroimaging data. *Nature Methods*, *8*(8), 665–670. https://doi.org/10.1038/nmeth.1635

Yen, C.-T., & Lu, P.-L. (2013). Thalamus and pain. *Acta Anaesthesiologica Taiwanica*, *51*(2), 73–80. https://doi.org/10.1016/j.aat.2013.06.011

FIGURE CAPTIONS

Figure 1. PRISMA flowchart for study inclusion.

Figure 2. Number of experiments included in each analysis of interest.

Figure 3. Main effect of experimental induction of acute pain. (A) Main effect of experiencing nociceptive pain across all 200 experiments (includes studies with the contrasts "pain > rest" and "pain > innocuous", as well as studies examining parametric modulation of pain. (B) Main effect of experiments with "pain > innocuous" contrast ($n = 62$). Coordinates and statistics for significant clusters are shown in **Table 2**.

Figure 4. Meta-analytic effect of experiments using "pain > rest" and "pain > innocuous" contrast. (A) Main effect of experiments using "pain > rest" contrast ($n = 134$). (B) Main effect of experiments with "pain > innocuous" contrast ($n = 62$). Coordinates and statistics for significant clusters are shown in **Table 3**.

Figure 5. The meta-analytic effects of thermal and non-thermal nociceptive pain induction. (A) Main effect of thermal pain experiments ($n = 107$). (B) Main effect of non-thermal pain experiments ($n = 98$). Coordinates and statistics for significant clusters associated with the main effect of thermal and non-thermal pain (as well as the between-experiment contrast and conjunction of thermal and non-thermal pain experiments) are shown in **Table 4**.

Figure 6. Effects of induction of electrically-evoked and mechanical nociceptive pain. (A) Main effect of electrically-evoked pain experiments ($n = 39$). (B) Main effect of mechanical pain experiments ($n = 46$). Coordinates and statistics for significant clusters associated with the main effect of electrical and mechanical pain (as well as the between-experiment contrast and conjunction of electrical and mechanical pain experiments) are shown in **Table 5**.

Figure 7. Main effect of meta-analysis of nociceptive chemical pain experiments ($n = 13$). Coordinates and statistics for significant clusters associated with the main effect of chemical pain are shown in **Table 6**.

Figure 8. The meta-analytic effects of left-sided and right-sided pain induction. (A) Main effect of left-sided pain experiments ($n = 92$). (B) Main effect of right-sided pain experiments ($n = 66$). Coordinates and statistics for significant clusters associated with the main effect of left-sided and right-sided pain (as well as the between-experiment contrast and conjunction of left-sided and right-sided pain experiments) are shown in **Table 7**.

Figure 9. The meta-analytic effects of distal and proximal nociceptive pain. (A) Main effect of experiments inducing acute nociceptive pain in the distal extremities ($n = 68$). (B) Main effect of experiments inducing pain in the proximal extremities ($n = 85$). Coordinates and statistics for significant clusters associated with the main effect of distal and proximal pain (as well as the between-experiment contrast and conjunction of distal and proximal pain experiments) are shown in **Table 8**.

Figure 10. The meta-analytic effects of visceral and non-visceral mechanical pain. (A) Main effect of visceral pain experiments ($n = 17$). (B) Main effect of non-visceral mechanical pain experiments ($n = 29$).

Coordinates and statistics for significant clusters associated with the main effect of visceral and non-visceral pain (as well as the between-experiment contrast and conjunction of visceral and non-visceral pain experiments) are shown in **Table 9**.

Figure 11. Effect of pain in males and females. (A) Main effect of experiments with an all-female sample ($n = 22$). (B) Main effect of experiments with an all-male sample ($n = 30$). Coordinates and statistics for significant clusters are shown in **Table 10**.

Figure 12. A core set of bran regions recruited by acute pain. This figure depicts the spatial consistency of above-threshold activation convergence cross all reported main effects meta-analyses. The value assigned to each voxel reflects the number of main effects analyses in which it was reported as significant. Values range from 1 (reported significant in only one main effects meta-analyses) to 15 (reported as significant in all main effects meta-analyses). The most consistently activated areas include bilateral thalamus, bilateral insula, bilateral SII, and bilateral MCC.

Supplementary Figure 1. PRISMA checklist for reporting of meta-analyses.

TABLES

Table 1. Number of experiments included and number of participants for each effect of interest.

Effect of interest	*n*	Total number of participants	Average number of participants
Nociceptive Pain			
All pain	200	3816	19
Pain > innocuous	62	1202	19
Pain > rest	134	2547	19
Modality			
Thermal	107	2083	19
Non-thermal	98	1801	18
Electrical	39	755	19
Mechanical	46	788	17
Chemical	13	258	20
Location			
Side			
Left	92	1873	20
Right	66	1214	18
Distal vs. Proximal Extremities			
Distal (hand or foot)	68	1254	18
Proximal (arm or leg)	85	1764	21
Visceral			
Visceral	17	262	15
Non-visceral mechanical	29	526	18
Sample sex			
All female	22	338	15
All male	30	533	18

Table 2. Peaks of convergence of activation for meta-analyses related to acute nociceptive pain.

Effect of Interest	Voxels	X	Y	Z	Macroanatomical Label	Cytoarchitectonic Label	*Z*-score
Main effect:							
Pain							
	14522	58	-24	22	R Supramarginal Gyrus	Area PFop (IPL)	8.52
	3181	6	12	38	R MCC		8.48
	325	-32	-56	-34	L Cerebellum	Lobule VI (Hem)	5.39
	238	48	4	42	R Precentral Gyrus		5.03

Note. Cluster coordinates are reported in MNI stereotaxic space. Macroanatomical labels used the SPM Anatomy Toolbox and Harvard-Oxford Structural Atlas (MCC = midcingulate cortex). Cytoarchitectonic labels were made using the SPM Anatomy Toolbox (IPL = inferior parietal lobe).

Table 3. Peaks of convergence of activation for meta-analyses related to acute nociceptive pain experiments using "pain > rest" contrast and "pain > innocuous" contrast.

Effect of Interest	Voxels	X	Y	Z	Macroanatomical Label	Cytoarchitectonic Label	*Z*-score
Main effect:							
Pain > rest							
	6936	58	-24	22	R Supramarginal Gyrus	Area PFop (IPL)	8.43
	4641	-34	18	4	L Insula Lobe		8.39
	2556	6	12	38	R MCC		8.37
	439	-10	-14	2	L Thalamus	Thal: Prefrontal	8.35
	164	-46	-40	44	L Inferior Parietal Lobule	Area hIP2 (IPS)	4.71
	135	-30	-56	-32	L Cerebellum (VI)	Lobule VI (Hem)	4.57
	134	48	4	38	R Precentral Gyrus		4.59
Main effect:							
Pain > innocuous							
	2301	38	8	6	R Insula Lobe		8.28
	2287	-38	-18	14	L Insula Lobe	Area Ig2	7.46
	1521	6	10	38	R MCC		7.58
	1005	10	-12	4	R Thalamus	Thal: Prefrontal	6.88

Note. Cluster coordinates are reported in MNI stereotaxic space. Macroanatomical labels used the SPM Anatomy Toolbox and Harvard-Oxford Structural Atlas (MCC = midcingulate cortex). Cytoarchitectonic labels were made using the SPM Anatomy Toolbox (IPL = inferior parietal lobe; Thal = thalamus).

Table 4. Peaks of convergence of activation for meta-analyses related to acute thermal and non-thermal nociceptive pain.

Effect of Interest	Voxels	X	Y	Z	Macroanatomical Label	Cytoarchitectonic Label	*Z*-score
Main effect: Thermal							
	9080	56	-24	22	R Rolandic Operculum	Area PFop (IPL)	8.4
	2161	4	12	38	R MCC		8.36
	571	44	44	6	R Middle Frontal Gyrus		7.81
	223	-32	-54	-34	L Cerebellum (VI)	Lobule VI (Hem)	5.2
	152	48	6	36	R Precentral Gyrus		5.32
Main effect: Non-thermal							
	4398	54	4	4	R Rolandic Operculum		8.31
	3874	-56	-20	18	L Postcentral Gyrus	Area OP1 [SII]	8.31
	2094	8	12	36	R MCC		7.53
	939	14	-14	4	R Thalamus	Thal: Prefrontal	8.32
	136	42	48	14	R Middle Frontal Gyrus		3.91
Thermal > non-thermal							
	55	2	6	40	R MCC		8.13
Non-thermal > thermal							
	46	44	0	-4	R Insula Lobe		3.67
	40	-40	-32	20	L Rolandic Operculum		3.86
Thermal AND non-thermal							
	2904	60	-24	22	R Supramarginal Gyrus	Area OP1 [SII]	8.29
	2674	-58	-22	18	L Supramarginal Gyrus	Area OP1 [SII]	8.3
	1506	8	12	36	R MCC		7.53
	327	14	-12	8	R Thalamus	Thal: Prefrontal	7.78
	263	-10	-14	2	L Thalamus	Thal: Prefrontal	7.81
	127	42	48	14	R Middle Frontal Gyrus		3.91

Note. Cluster coordinates are reported in MNI stereotaxic space. Macroanatomical labels were made using the SPM Anatomy Toolbox and Harvard-Oxford Structural Atlas (MCC = midcingulate cortex). Cytoarchitectonic labels were made using the SPM Anatomy Toolbox only (IPL = inferior parietal lobe; Thal = thalamus).

Table 5. Peaks of convergence of activation for meta-analyses related to acute electrical and mechanical nociceptive pain.

Effect of Interest	Voxels	X	Y	Z	Macroanatomical Label	Cytoarchitectonic Label	Z-score
Main effect: Electrical							
	1901	54	2	6	R Rolandic Operculum		7.52
	1514	-56	-20	20	L Postcentral Gyrus	Area OP1 [SII]	6.17
	729	10	12	38	R MCC		4.87
	249	14	-16	6	R Thalamus	Thal: Prefrontal	6.59
	202	-12	-16	8	L Thalamus	Thal: Prefrontal	5.27
Main effect: mechanical							
	1354	34	6	8	R Insula Lobe		5.63
	848	-44	0	6	L Insula Lobe		5.19
	814	-54	-22	16	L Supramarginal Gyrus	Area OP1 [SII]	7.39
	755	58	-26	24	R Supramarginal Gyrus	Area PFop (IPL)	7.46
	501	4	14	34	R MCC		5.7
	227	-12	-14	4	L Thalamus	Thal: Prefrontal	6.76
	164	12	-12	2	R Thalamus	Thal: Prefrontal	6.9
Electrical > mechanical							
	33	44	-20	22	R Rolandic Operculum		3.83
	26	6	-18	10	R Thalamus	Thal: Temporal	3.54
	25	46	2	-16	R Superior Temporal Gyrus		3.45
Mechanical > electrical							
					No suprathreshold clusters		
Electrical AND mechanical							
	466	36	6	10	R Insula Lobe		4.76
	462	-56	-20	18	L Postcentral Gyrus	Area OP1 [SII]	6.06
	334	60	-22	20	R Supramarginal Gyrus	Area OP1 [SII]	5.47
	275	-36	4	12	L Insula Lobe		5.05
	243	8	14	36	R MCC		4.62
	113	-14	-16	8	L Thalamus	Thal: Prefrontal	5.01
	98	14	-14	6	R Thalamus	Thal: Prefrontal	5.8

Note. Cluster coordinates are reported in MNI stereotaxic space. Macroanatomical labels were made using the SPM Anatomy Toolbox and Harvard-Oxford Structural Atlas (MCC = midcingulate cortex). Cytoarchitectonic labels were made using the SPM Anatomy Toolbox only (Thal = thalamus).

Table 6. Peaks of convergence of activation for meta-analyses related to acute nociceptive chemical pain

Voxels	X	Y	Z	Macroanatomical Label	Cytoarchitectonic Label	Z-score
663	38	16	-6	R Insula Lobe		5.29
534	-58	-4	8	L Rolandic Operculum	Area OP4 [PV]	4.78
449	62	-14	20	R Postcentral Gyrus	Area PFop (IPL)	4.43
329	-10	12	38	L MCC		5.22
232	-34	10	2	L Insula Lobe		5.26
183	-2	-2	62	L SMA		4.85
163	14	-14	6	R Thalamus	Thal: Prefrontal	5.35
154	-12	-20	-4	L Thalamus	Thal: Motor	5.19
117	-6	-40	-50	Brainstem		5.19
105	-36	-8	4	L Insula Lobe		4.1

Note. Cluster coordinates are reported in MNI stereotaxic space. Macroanatomical labels were made using the SPM Anatomy Toolbox and Harvard-Oxford Structural Atlas (SMA = supplementary motor area). Cytoarchitectonic labels were made using the SPM Anatomy Toolbox (IPL = inferior parietal lobe; Thal = thalamus).

Table 7. Peaks of convergence of activation for meta-analyses related to left-sided and right-sided acute nociceptive pain.

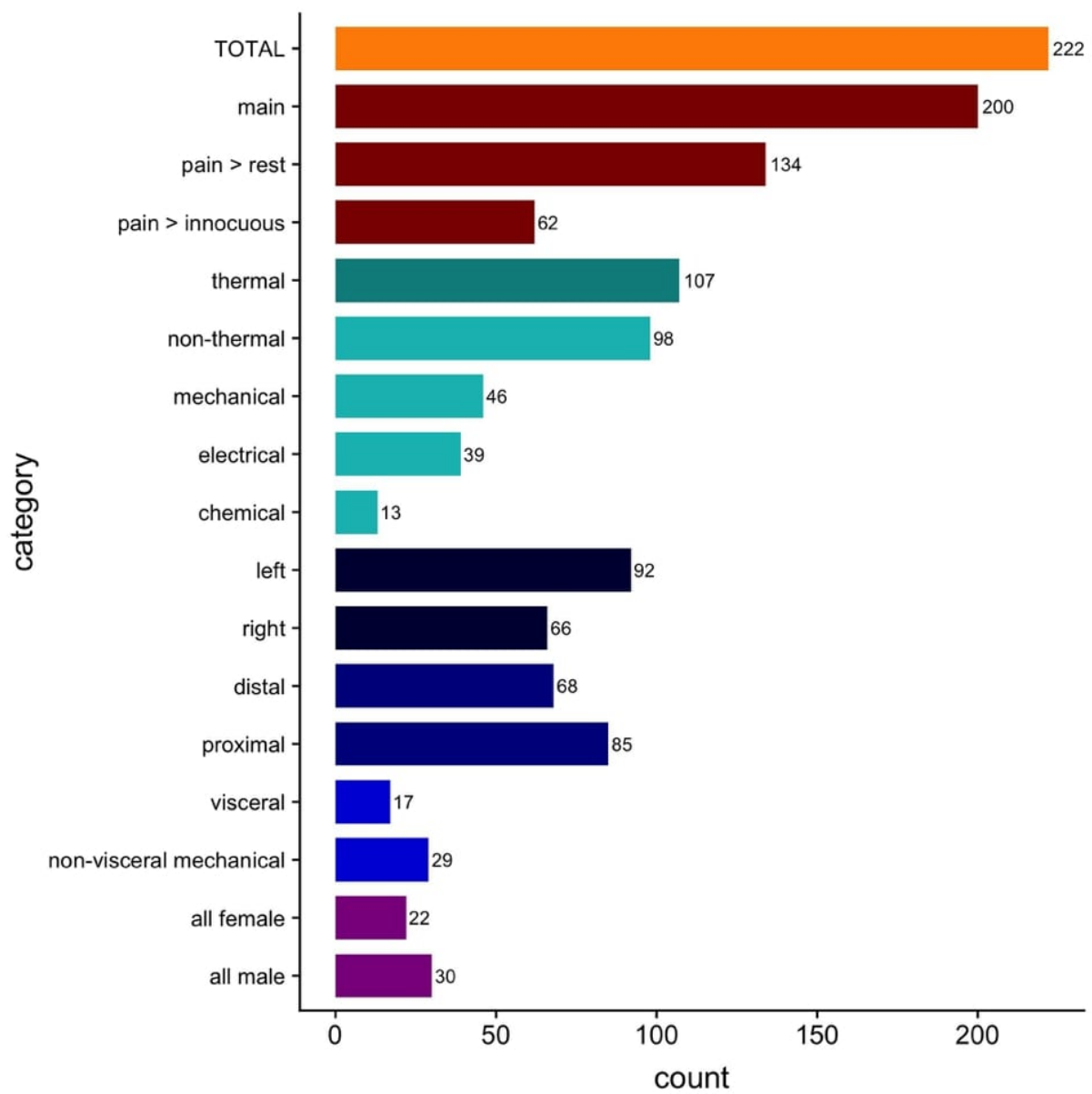| Effect of Interest	Voxels	X	Y	Z	Macroanatomical Label	Cytoarchitectonic Label	Z-score
Main effect: Left							
	5034	40	-16	16	R Rolandic Operculum	Area OP3 [VS]	8.34
	3096	-60	-24	20	L Supramarginal Gyrus	Area PFop (IPL)	8.31
	1445	6	12	38	R MCC		8.29
	236	44	44	6	R Middle Frontal Gyrus		5.73
	137	-32	-56	-32	L Cerebellum (VI)	Lobule VI (Hem)	4.62
	125	24	-44	68	R Postcentral Gyrus	Area 1	5.87
Main effect: Right							
	2944	-40	-18	14	L Rolandic Operculum	Area Ig2	8.27
	1743	38	20	4	R Insula Lobe		7.61
	1737	6	12	38	R MCC		7.63
	689	58	-22	22	R Supramarginal Gyrus	Area PFop (IPL)	8.28
	301	44	44	6	R Middle Frontal Gyrus		5.99
	224	-12	-14	4	L Thalamus	Thal: Prefrontal	6.16
	217	50	2	44	R Precentral Gyrus		5.31
	170	14	-14	6	R Thalamus	Thal: Prefrontal	5.06
	143	52	-38	46	R Inferior Parietal Lobule	Area PFm (IPL)	4.1
Left > right							
	No suprathreshold clusters						
Right > left							
	45	-44	-22	16	L Rolandic Operculum	Area OP1 [SII]	6.8
Left AND right							
	1437	-32	18	6	L Insula Lobe		7.11
	1318	38	20	0	R Insula Lobe		6.76
	1116	6	12	38	R MCC		7.63
	608	58	-22	22	R Supramarginal Gyrus	Area PFop (IPL)	8.28
	542	-58	-26	20	L Supramarginal Gyrus	Area PFop (IPL)	8.08
	178	44	44	6	R Middle Frontal Gyrus		5.73
	167	14	-14	6	R Thalamus	Thal: Prefrontal	5.06
	158	-12	-14	4	L Thalamus	Thal: Prefrontal	6.16

Note. Cluster coordinates are reported in MNI stereotaxic space. Macroanatomical labels were made using the SPM Anatomy Toolbox and Harvard-Oxford Structural Atlas (MCC = midcingulate cortex).

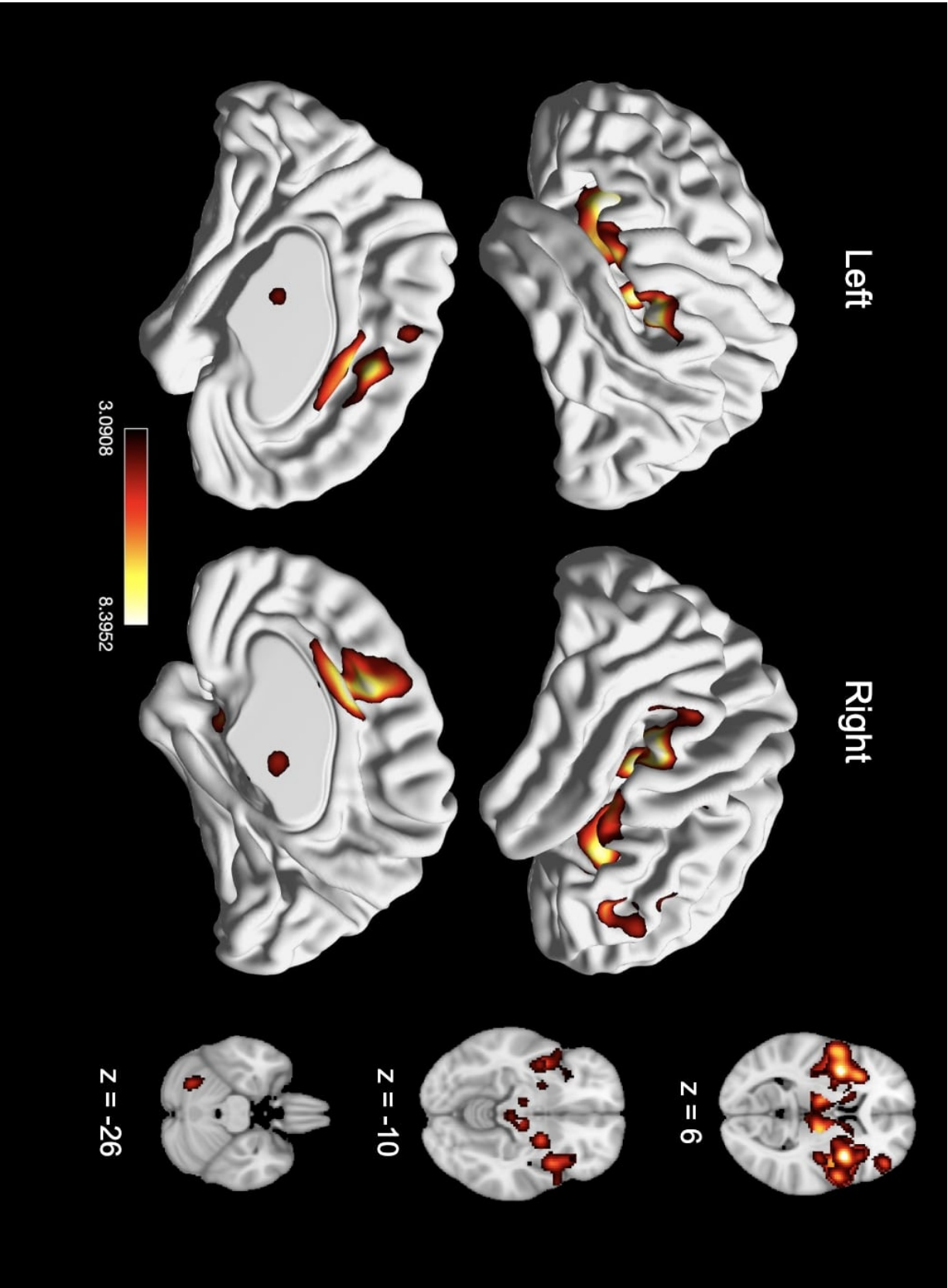Cytoarchitectonic labels were made using the SPM Anatomy Toolbox only (IPL = inferior parietal lobe; Thal = thalamus; VS = ventral somatosensory).

Table 8. Peaks of convergence of activation for meta-analyses related to distal and proximal acute nociceptive pain.

Effect of Interest	Voxels	X	Y	Z	Macroanatomical Label	Cytoarchitectonic Label	Z-score
Main effect: Distal							
	3044	56	-26	22	R Rolandic Operculum	Area PFop (IPL)	8.3
	2579	-60	-24	20	L Supramarginal Gyrus	Area PFop (IPL)	8.28
	1384	4	10	38	R MCC		6.46
	605	12	-12	4	R Thalamus	Thal: Prefrontal	6.68
	222	46	42	6	R Middle Frontal Gyrus		4.72
	162	-10	-12	2	L Thalamus	Thal: Prefrontal	6.21
Main effect: Proximal							
	4319	38	-18	16	R Rolandic Operculum	Area OP2 [PIVC]	8.32
	3261	-36	4	8	L Insula Lobe		8.31
	1696	6	12	38	R MCC		8.31
	227	44	44	6	R Middle Frontal Gyrus		6.05
	223	48	6	38	R Precentral Gyrus		5.62
	182	22	-44	68	R Postcentral Gyrus	Area 1	6.5
Distal > proximal							
					No suprathreshold clusters		
Proximal > distal							
					No suprathreshold clusters		
Distal AND proximal							
	2041	56	-24	22	R Rolandic Operculum	Area PFop (IPL)	8.3
	1156	-34	20	4	L Insula Lobe		7.25
	917	4	10	38	R MCC		6.46
	854	-60	-24	20	L Supramarginal Gyrus	Area PFop (IPL)	8.28
	258	12	-12	4	R Thalamus	Thal: Prefrontal	6.68
	153	-10	-12	2	L Thalamus	Thal: Prefrontal	6.21
	97	46	42	6	R Middle Frontal Gyrus		4.69
	77	16	4	0	R Pallidum		4.01

Note. Cluster coordinates are reported in MNI stereotaxic space. Macroanatomical labels were made using the SPM Anatomy Toolbox and Harvard-Oxford Structural Atlas (MCC = midcingulate cortex). Cytoarchitectonic labels were made using the SPM Anatomy Toolbox only (IPL = inferior parietal lobe; Thal = thalamus).
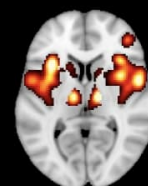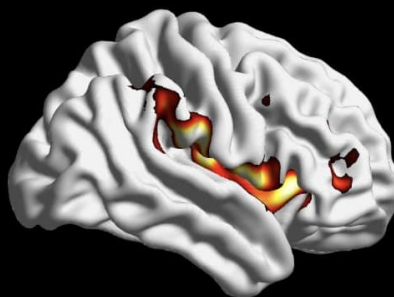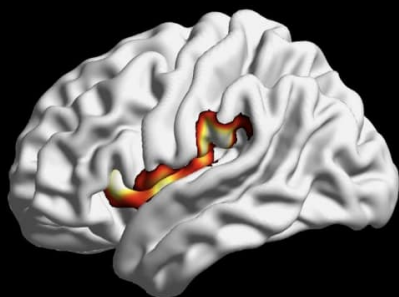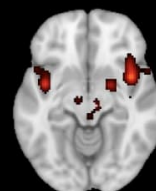
Table 9. Peaks of convergence of activation for meta-analyses related to acute visceral and non-visceral nociceptive pain.

Effect of Interest	Voxels	X	Y	Z	Macroanatomical Label	Cytoarchitectonic Label	Z-score
Main effect: Visceral							
	431	60	-24	26	R Supramarginal Gyrus	Area PFop (IPL)	6.14
	237	-32	0	-2	L Putamen		4.76
	174	54	-6	8	R Rolandic Operculum	Area OP4 [PV]	4.66
	142	-8	-14	-2	L Thalamus	Thal: Prefrontal	4.89
	91	8	16	36	R MCC		4.2
Main effect: Non-visceral mechanical							
	606	-56	-24	18	L Supramarginal Gyrus	Area OP1 [SII]	5.93
	394	-44	2	4	L Insula Lobe		5.24
	351	60	-22	18	R Supramarginal Gyrus	Area OP1 [SII]	5.71
	272	4	14	34	R MCC		4.71
	185	44	18	0	R Insula Lobe		4.59
	150	54	8	6	R Rolandic Operculum	Area 44	4.31
	140	36	6	6	R Insula Lobe		4.87
	128	20	14	4	R Caudate		4.38
	108	-14	-14	4	L Thalamus	Thal: Prefrontal	5.52
	100	14	-12	4	R Thalamus	Thal: Prefrontal	5
Visceral > Non-visceral mechanical							
	No suprathreshold clusters						
Non-visceral mechanical > visceral							
	No suprathreshold clusters						
Visceral AND Non-visceral mechanical							
	136	58	-28	24	R Supramarginal Gyrus	Area PFcm (IPL)	5.18
	74	-10	-14	2	L Thalamus	Thal: Prefrontal	4.49

Note. Cluster coordinates are reported in MNI stereotaxic space. Macroanatomical labels were made using the SPM Anatomy Toolbox and Harvard-Oxford Structural Atlas (MCC = midcingulate cortex). Cytoarchitectonic labels were made using the SPM Anatomy Toolbox only (IPL = inferior parietal lobe; Thal = thalamus).

Table 10. Peaks of convergence of activation for meta-analyses related to all-female and all-male samples.

Effect of Interest	Voxels	X	Y	Z	Macroanatomical Label	Cytoarchitectonic Label	Z-score
Main effect: Female							
	315	-32	16	8	L Insula Lobe		6.36
	249	-64	-28	22	L Superior Temporal Gyrus	Area PFop (IPL)	5.02
	213	38	16	-2	R Insula Lobe		4.48
	142	-40	-4	0	L Insula Lobe		4.27
	98	62	-20	24	R Supramarginal Gyrus	Area PFt (IPL)	4.98
Main effect: Male							
	1115	-34	20	0	L Insula Lobe		6.76
	547	8	14	36	R MCC		6.39
	477	36	22	2	R Insula Lobe		6.52
	374	56	12	-4	R Temporal Pole	Area TE 3	5.03
	305	56	-26	22	R Rolandic Operculum	Area PFop (IPL)	4.87
	274	44	46	4	R Middle Frontal Gyrus		6.05
	189	-10	-12	4	L Thalamus	Thal: Prefrontal	5.98
	169	14	-14	8	R Thalamus	Thal: Prefrontal	5.59
Female > male							
	No suprathreshold clusters						
Male > female							
	No suprathreshold clusters						
Female AND male							
	141	-62	-26	22	L Supramarginal Gyrus	Area PFop (IPL)	4.88
	88	-32	18	4	L Insula Lobe		5.13
	58	38	18	-2	R Insula Lobe		4.14

Note. Cluster coordinates are reported in MNI stereotaxic space. Macroanatomical labels were made using the SPM Anatomy Toolbox and Harvard-Oxford Structural Atlas (MCC = midcingulate cortex). Cytoarchitectonic labels were made using the SPM Anatomy Toolbox only (IPL = inferior parietal lobe; Thal = thalamus).

| Identification | **Records identified through database search** n=7529 | **Additional records identified through other sources** references from reviews, n=1216 |

Records after duplicates removed n=4927

| Screening | **Records screened** n=4927 | **Records excluded** n=3750 |

| Eligibility | **Full-text articles assessed for eligibility** n=1177 | **Full-text articles excluded** Full-text not available in English n=15, Insufficient sample size n=141, Not peer-reviewed journal article n=5, Not experimental n=221, No confirmed pain induction n=89, Healthy volunteers data not available n=21, Animal study n=5, No usable pain contrast n=172, Not BOLD fMRI n=140, Not whole brain search n=102, Statistical threshold not met or insufficient detail n=28, Data not available n=38 |

| Included | **Articles included in quantitative synthesis (meta-analysis)** n=200 (n=222 fMRI experiments) |

Left

Right

3.0908

8.3952

z = -26

z = -10

z = 6

A

Left   Right

z = 6

z = -10

z = -26

3.1001   8.4278

B

z = 2

z = -8

3.1004   8.2827

A

Left   Right

z = 6

z = -8

3.0908   8.3952

z = -30

B

z = 0

z = -10

3.1018   8.3246

Left   Right
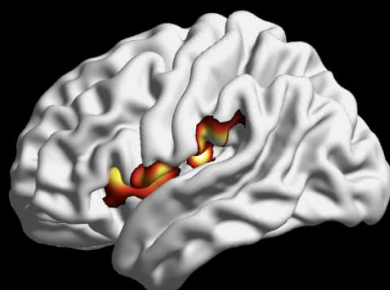
A

3.1039   7.5188

z = 8

B

3.1026   7.4569

z = 4

Left

Right

3.1083

5.3496

z = -47

z = 2

A

Left　　　　　Right

z = 4

z = -16

3.0932　　8.2994

B

z = 2

z = -2

3.1003　　8.3189

A

Left   Right

z = 4

3.0963   6.1381

B

z = 4

3.1003   5.9252

A

Left Right

z = 4

3.0919 6.7563

B

z = 8

3.1090 6.3590

Left

Right

z = -26

z = -10

z = 6

PRISMA 2009 Checklist

Section/topic	#	Checklist item	Reported on page #
TITLE			
Title	1	Identify the report as a systematic review, meta-analysis, or both.	1
ABSTRACT			
Structured summary	2	Provide a structured summary including, as applicable: background; objectives; data sources; study eligibility criteria, participants, and interventions; study appraisal and synthesis methods; results; limitations; conclusions and implications of key findings; systematic review registration number.	2
INTRODUCTION			
Rationale	3	Describe the rationale for the review in the context of what is already known.	3
Objectives	4	Provide an explicit statement of questions being addressed with reference to participants, interventions, comparisons, outcomes, and study design (PICOS).	3
METHODS			
Protocol and registration	5	Indicate if a review protocol exists, if and where it can be accessed (e.g., Web address), and, if available, provide registration information including registration number.	5
Eligibility criteria	6	Specify study characteristics (e.g., PICOS, length of follow-up) and report characteristics (e.g., years considered, language, publication status) used as criteria for eligibility, giving rationale.	supplementary
Information sources	7	Describe all information sources (e.g., databases with dates of coverage, contact with study authors to identify additional studies) in the search and date last searched.	5-6
Search	8	Present full electronic search strategy for at least one database, including any limits used, such that it could be repeated.	5
Study selection	9	State the process for selecting studies (i.e., screening, eligibility, included in systematic review, and, if applicable, included in the meta-analysis).	8
Data collection process	10	Describe method of data extraction from reports (e.g., piloted forms, independently, in duplicate) and any processes for obtaining and confirming data from investigators.	8-9
Data items	11	List and define all variables for which data were sought (e.g., PICOS, funding sources) and any assumptions and simplifications made.	supplementary
Risk of bias in individual studies	12	Describe methods used for assessing risk of bias of individual studies (including specification of whether this was done at the study or outcome level), and how this information is to be used in any data synthesis.	NA
Summary measures	13	State the principal summary measures (e.g., risk ratio, difference in means).	10
Synthesis of results	14	Describe the methods of handling data and combining results of studies, if done, including measures of consistency (e.g., I²) for each meta-analysis.	10

PRISMA 2009 Checklist

Section/topic	#	Checklist item	Reported on page #
Risk of bias across studies	15	Specify any assessment of risk of bias that may affect the cumulative evidence (e.g., publication bias, selective reporting within studies).	13
Additional analyses	16	Describe methods of additional analyses (e.g., sensitivity or subgroup analyses, meta-regression), if done, indicating which were pre-specified.	12-13
RESULTS			
Study selection	17	Give numbers of studies screened, assessed for eligibility, and included in the review, with reasons for exclusions at each stage, ideally with a flow diagram.	13-14
Study characteristics	18	For each study, present characteristics for which data were extracted (e.g., study size, PICOS, follow-up period) and provide the citations.	supplementary
Risk of bias within studies	19	Present data on risk of bias of each study and, if available, any outcome level assessment (see item 12).	NA
Results of individual studies	20	For all outcomes considered (benefits or harms), present, for each study: (a) simple summary data for each intervention group (b) effect estimates and confidence intervals, ideally with a forest plot.	supplementary
Synthesis of results	21	Present results of each meta-analysis done, including confidence intervals and measures of consistency.	14
Risk of bias across studies	22	Present results of any assessment of risk of bias across studies (see Item 15).	14
Additional analysis	23	Give results of additional analyses, if done (e.g., sensitivity or subgroup analyses, meta-regression [see Item 16]).	15-20
DISCUSSION			
Summary of evidence	24	Summarize the main findings including the strength of evidence for each main outcome; consider their relevance to key groups (e.g., healthcare providers, users, and policy makers).	21
Limitations	25	Discuss limitations at study and outcome level (e.g., risk of bias), and at review-level (e.g., incomplete retrieval of identified research, reporting bias).	26-27
Conclusions	26	Provide a general interpretation of the results in the context of other evidence, and implications for future research.	27
FUNDING			
Funding	27	Describe sources of funding for the systematic review and other support (e.g., supply of data); role of funders for the systematic review.	28

For more information, visit: **www.prisma-statement.org**.

Supplementary Table 1. Experimental contributions to each significant cluster in main effect of all studies inducing pain (n = 200)

Cluster	Experiments
Cluster 1: 14522 voxels (58, -24, 22)	
	Ando 2016
	Ariji 2018
	Asghar 2015
	Asghar 2016
	Atlas 2010
	Atlas 2014
	Baliki 2006
	Baliki 2009a
	Baliki 2010
	Bar 2007
	Becker 2017
	Benson 2012
	Bingel 2007a
	Bogdanov 2015
	Boland 2014
	Bouhassira 2013
	Boyle 2007
	Brinkmeyer 2010
	Brooks 2017
	Brugger 2011
	Brugger 2012
	Choi 2011
	Choi 2016
	Cleve 2017
	Coen 2008
	Coen 2009
	Coen 2011
	Cole 2006
	Cole 2010
	Corradi-Dell' Acqua 2011
	Davis 2016
	De la Fuente-Sandoval 2010
	De la Fuente-Sandoval 2012
	Dobek 2014
	Downar 2003
	Dube 2009

Dunckley 2005a
Eisenblatter 2017
Elsenbruch 2009
Esser 2017
Ettlin 2009
Farmer 2013
Farrell 2012
Farrell 2014
Fehse 2015
Forkmann 2013
Frankenstein 2001
Freund 2007
Freund 2009
Gard 2012
Geuze 2007
Godinho 2012
Gracely 2002
Grant 2011
Gu 2016
Guleria 2017
Gundel 2008
Habig 2017
Hahn 2013
Hansen 2015
Heckel_2011
Hu 2015
Iannilli 2008
Ibinson 2013
Jahn 2016
Jensen 2015
Kamping 2016
Kattoor 2013
Kim 2013b
Kobuch 2017
Kobuch 2018
Kong 2006
Kong 2010
Koyama 2005
Kross 2011
LaCesa 2014

Ladabaum 2007

Landgrebe 2008

Lee 2008

Lee 2015

Leung 2016a

Lindstedt 2011

Lloyd 2008

Loggia 2012

Loggia 2014

Loken 2017

Longo 2012

Lopez-Sola 2010a

Lopez-Sola 2010b

Lu 2004

Lui 2008

Lutz 2013

Lynn 2016

Maeda 2011

Maihofner 2004

Maihofner 2005

Maihofner 2006

Maihofner 2011

Mainero 2007

Markl 2013

Martin 2013

Mayhew 2013

Meier 2015

Misra 2015

Moana-Filho 2015

Mobascher 2009a

Mobascher 2009b

Mobascher 2010a

Mobascher 2010b

Mochizuki 2007

Mohr 2008

Moisset 2010

Morrison 2004

Moulton 2011

Moulton 2012

Naglatzki 2012

Nickel 2014
Niddam 2002
Obermann 2009
Ochsner 2006
Oertel 2008
Oertel 2012
Orenius 2017
Oshiro 2007
Oshiro 2009
Pazmany 2017
Peltz 2011
Perini 2013
Perlaki 2015
Perrotta 2017
Petschow 2016
Piche 2010
Pogatzki-Zahn 2010
Pujol 2017
Quiton 2014
Roberts 2008
Rodriguez-Raecke 2010
Rosenberger 2009
Rottmann 2010
Roy 2009
Rubio 2015
Russo 2012
Rutgen 2015
Salomons 2015
Scheef 2012
Schenk 2017
Schmahl 2006
Schoell 2010
Schulte 2016
Schulz-Stubner 2004
Seidel 2015
Seifert 2007
Seminowicz 2006
Seminowicz 2007
Sevel 2015
Shelton 2012

Shenoy 2011
Shinozaki 2016
Sinke 2016
Sinke 2017
Smith 2011
Song 2006
Sprenger 2015
Sprenger 2018
Stammler 2008
Stankewitz 2010
Starr 2009
Stoeckel 2016
Strigo 2013a
Strigo 2013b
Takahashi 2011
Talmi 2009
Tan 2015
Tedeschi 2015
Tessitore 2017
Theysohn 2014
Tseng 2010
Tseng 2013
Tseng 2015
Tseng 2017
Vachon-Presseau 2013
van den Bosch 2013
Vanhaudenhuyse 2009
von Leupoldt 2008
von Leupoldt 2009
Wagner 2009
Weiss 2008
Wiech 2005
Wiech 2006
Wiech 2009
Wiech 2010
Winston 2014
Woo 2015
Yang 2012
Yang 2018
Yoshino 2010

Youssef 2016
Zeidan 2015
Ziv 2010

Cluster 2: 3181 voxels (6, 12, 38)

Ando 2016
Asghar 2015
Asghar 2016
Atlas 2010
Atlas 2014
Baliki 2006
Baliki 2009a
Baliki 2010
Becker 2017
Benson 2012
Bogdanov 2015
Boland 2014
Brinkmeyer 2010
Brooks 2017
Brugger 2011
Choi 2011
Choi 2016
Coen 2008
Coen 2009
Coen 2011
Cole 2006
Cole 2010
Corradi-Dell' Acqua 2011
Davis 2016
De la Fuente-Sandoval 2010
De la Fuente-Sandoval 2012
Dobek 2014
Downar 2003
Dube 2009
Dunckley 2005a
Eisenblatter 2017
Esser 2017
Ettlin 2009
Farmer 2013
Farrell 2012
Farrell 2014

Fehse 2015

Ferris 2016

Forkmann 2013

Frankenstein 2001

Freund 2009

Gard 2012

Geuze 2007

Godinho 2012

Gracely 2002

Grant 2011

Guleria 2017

Gundel 2008

Habig 2017

Hansen 2015

Hu 2015

Iannilli 2008

Ibinson 2013

Jahn 2016

Jensen 2015

Kamping 2016

Kobuch 2017

Kobuch 2018

Kong 2006

Kong 2010

Koyama 2005

Kross 2011

Ladabaum 2007

Landgrebe 2008

Lee 2008

Loggia 2012

Longo 2012

Lopez-Sola 2010a

Lopez-Sola 2010b

Lu 2004

Lui 2008

Lutz 2013

Lynn 2016

Maeda 2011

Maihofner 2006

Maihofner 2011

Mainero 2007
Markl 2013
Martin 2013
Mayhew 2013
Misra 2015
Mobascher 2009a
Mobascher 2009b
Mobascher 2010a
Mobascher 2010b
Mochizuki 2007
Mohr 2008
Morrison 2004
Moulton 2011
Moulton 2012
Naglatzki 2012
Nickel 2014
Niddam 2002
Obermann 2009
Ochsner 2006
Oertel 2008
Oertel 2012
Oshiro 2007
Oshiro 2009
Peltz 2011
Perlaki 2015
Perrotta 2017
Petschow 2016
Piche 2010
Pujol 2017
Quiton 2014
Roberts 2008
Rodriguez-Raecke 2010
Rottmann 2010
Roy 2009
Russo 2012
Rutgen 2015
Salomons 2015
Scheef 2012
Schenk 2017
Schmahl 2006

Schulz-Stubner 2004

Seminowicz 2006

Seminowicz 2007

Sevel 2015

Shelton 2012

Shenoy 2011

Shinozaki 2016

Sinke 2016

Sinke 2017

Song 2006

Sprenger 2015

Sprenger 2018

Stankewitz 2010

Starr 2009

Stoeckel 2016

Strigo 2013b

Takahashi 2011

Talmi 2009

Tan 2015

Tedeschi 2015

Tessitore 2017

Theysohn 2014

Tseng 2013

Tseng 2015

Tseng 2017

Vachon-Presseau 2013

Vanhaudenhuyse 2009

von Leupoldt 2008

von Leupoldt 2009

Wagner 2009

Weiss 2008

Wiech 2005

Wiech 2010

Winston 2014

Woo 2015

Yang 2012

Yang 2018

Yoshino 2010

Youssef 2016

Zeidan 2015

Ziv 2010

Cluster 3: 325 voxels (-32, -56, -34)

Ariji 2018
Asghar 2015
Bar 2007
Benson 2012
Bogdanov 2015
Boland 2014
Boyle 2007
Brooks 2017
Corradi-Dell' Acqua 2011
Dobek 2014
Dube 2009
Farrell 2012
Farrell 2014
Gracely 2002
Hahn 2013
Hansen 2015
Jahn 2016
Kamping 2016
Kim 2013b
Kong 2010
Kross 2011
Lee 2008
Loggia 2014
Lopez-Sola 2010a
Lu 2004
Mobascher 2009a
Mobascher 2010a
Mobascher 2010b
Mohr 2008
Nickel 2014
Oshiro 2009
Roy 2009
Rutgen 2015
Scheef 2012
Shelton 2012
Shenoy 2011
Shinozaki 2016
Song 2006

Sprenger 2015
Sprenger 2018
Starr 2009
Stoeckel 2016
Strigo 2013b
Takahashi 2011
Tedeschi 2015
Weiss 2008
Winston 2014
Woo 2015
Youssef 2016

Cluster 4: 238 voxels (48, 4, 42)

Boyle 2007
Brooks 2017
Choi 2011
Coen 2011
Cole 2006
Cole 2010
Dube 2009
Farmer 2013
Farrell 2012
Farrell 2014
Freund 2007
Gard 2012
Geuze 2007
Iannilli 2008
Kong 2010
Kross 2011
Ladabaum 2007
Landgrebe 2008
Loggia 2012
Longo 2012
Lopez-Sola 2010a
Maihofner 2005
Maihofner 2006
Maihofner 2011
Mayhew 2013
Misra 2015
Moisset 2010
Moulton 2011

Ochsner 2006
Oshiro 2009
Peltz 2011
Piche 2010
Quiton 2014
Russo 2012
Salomons 2015
Scheef 2012
Schmahl 2006
Shinozaki 2016
Stoeckel 2016
Takahashi 2011
Tseng 2010
Tseng 2015
von Leupoldt 2009
Wagner 2009
Winston 2014
Ziv 2010

Note: Cluster identification on the first column indicates cluster number, number of voxels in cluster, and peak coordinate of cluster.

Supplementary Table 2. PICOS table for search and eligibility criteria.

Concept	Keyword/Synonyms
P – Population	Healthy participants over the age of 18
I - Intervention, Prognostic Factor, or Exposure	Confirmed physical pain induction ("pain" or "noxious" or "nociception")
C - Comparison or Intervention	*Not applicable*
O - Outcome	Reported MNI or Talairach coordinate results from BOLD response to pain measured by task-induced fMRI ("MRI" or "magnetic resonance imaging" or "fMRI" or "BOLD" or "brain mapping")
S - Study	1. Includes at least 10 participants 2. Conducts a whole brain search 3. Meets statistical threshold of voxel height of $p < 0.001$ uncorrected or cluster-corrected height of p < 0.05 for cluster identification